

8-2017

# Novel Anti-Obesity Effects of Beer Hops Compound Xanthohumol: Role of Ampk Signaling Pathway

Janaiya S Samuels

*Philadelphia College of Osteopathic Medicine*

Follow this and additional works at: <http://digitalcommons.pcom.edu/biomed>

 Part of the [Medicine and Health Sciences Commons](#)

---

## Recommended Citation

Samuels, Janaiya S, "Novel Anti-Obesity Effects of Beer Hops Compound Xanthohumol: Role of Ampk Signaling Pathway" (2017).  
*PCOM Biomedical Studies Student Scholarship*. 138.  
<http://digitalcommons.pcom.edu/biomed/138>

This Thesis is brought to you for free and open access by the Student Dissertations, Theses and Papers at DigitalCommons@PCOM. It has been accepted for inclusion in PCOM Biomedical Studies Student Scholarship by an authorized administrator of DigitalCommons@PCOM. For more information, please contact [library@pcom.edu](mailto:library@pcom.edu).

NOVEL ANTI-OBESITY EFFECTS OF BEER HOPS  
COMPOUND XANTHOTHUMOL: ROLE OF AMPK  
SIGNALING PATHWAY

A Thesis Presented to the Philadelphia College of Osteopathic Medicine –  
Georgia Campus

In Partial Fulfillment for the Degree of

Master of Science

August 2017

Janaiya S. Samuels

Advisor: Dr. Srujana Rayalam

This thesis has been presented to and accepted by the Associate Dean for Curriculum and Research Office for Philadelphia College of Osteopathic Medicine – Georgia Campus in partial fulfillment of the requirements for the degree of Master of Science in Biomedical Sciences.

We the undersigned duly appointed committee have read and examined this manuscript and certify it is adequate in scope and quality as a thesis for this master's degree. We approve the content of the thesis to be submitted for processing and acceptance

---

Srujana Rayalam, Ph.D.  
Assistant Professor of Pharmaceutical Sciences  
Thesis Advisor

---

Date of Signature

---

Rangaiah Shashidharamurthy, Ph.D.  
Assistant Professor of Pharmaceutical Sciences

---

Date of Signature

---

Vicky Mody, Ph.D.  
Associate Professor of Pharmaceutical Sciences

---

Date of Signature

---

Harold Komiskey, Ph.D.  
Associate Professor of Neuroscience, Physiology and Pharmacology

---

Date of Signature

---

Richard White, Ph.D.  
Associate Director, Graduate Program in Biomedical Sciences  
Professor of Neuroscience, Physiology and Pharmacology

---

Date of Signature

## Acknowledgements

I would like to extend my most sincere gratitude to Dr. Srujana Rayalam, my thesis advisor and mentor, for welcoming me as her graduate student. Dr. Rayalam has been instrumental in my growth as a future scientist and has molded me into a life-long learner. My commitment to research is contributed to your dedication to me as a former graduate student. Thank you.

To my thesis committee, Drs. Murthy, Mody, and Komiskey, thank you for always pushing me to be better than I was yesterday. Thank you for investing your time and expertise into me. Thank you for all for the beneficial feedback and support throughout this past year.

## **Abstract**

Obesity, a chronic disease, is a global epidemic that affects millions of lives and increases the risk of several comorbidities such as Type 2 diabetes, musculoskeletal disorders, cardiovascular disease, and cancer. Obesity is the leading cause of death globally, and is associated with an excessive accumulation of white adipose tissue (WAT). Although obesity is a serious condition, safe, long-term drug therapies are limited. A second type of adipose tissue is known as brown adipose tissue (BAT), which functions as an energy dissipater in the form of heat, as opposed to energy storing WAT. Previous research has shown that the mitochondrial uncoupling protein 1 (UCP1), activates the thermogenic properties of BAT [1]. WAT lacks the expression of UCP1 and therefore has no protective mechanisms against obesity and stores energy in the form of triglycerides. Thermogenic BAT has been identified in adult humans [2], as such, this discovery has been an attractive target for anti-obesity therapy. Recently, studies have suggested that WAT can be transdifferentiated into brown-like beige adipose tissue (BeAT). This transdifferentiation process is referred to as “beiging” and is mediated by the activation of the sympathetic nervous system. Activation of BeAT, similar to BAT, generates heat at the expense of ATP. Additionally, immune cells like macrophages play an important role in the induction of thermogenesis in WAT and contribute to the beiging of WAT [3].

Current treatments for obesity, as well as “browning” agents, propose their own risks to humans and are not ideal long-term solutions for anti-obesity therapy. Consequently, many phytochemicals have been explored for their safe anti-obesity effects and as browning agents. Recently, xanthohumol (XN), a prenylated flavonoid found in Hops flowers, has been reported to inhibit adipogenesis and stimulate the apoptosis of adipocytes [4]. However, there are no published studies demonstrating the effects of XN on thermogenesis. In this current study, we will explore novel anti-obesity effects of XN to propose a multi-faceted approach for prevention and treatment of obesity. We propose to investigate the direct and indirect effects of XN on the induction of beiging in white adipocytes. Furthermore, we will investigate the role of adenosine monophosphate activated kinase (AMPK) signaling pathway in the induction of beiging.

The *in vitro* cell culture models utilized in this study are murine adipocyte (3T3-L1) and macrophage (RAW264.7) cell lines. Cell viability assay, Western blotting, ELISA, MitoTracker Green™, Oil Red O staining, AdipoRed™ assay, and a Transwell co-culturing system are employed to demonstrate the effects of XN on beiging and the role of AMPK pathway in XN-induced beiging. Our data suggests that XN has the ability to directly induce transdifferentiation of white to beige adipocytes and indirectly induce beiging by activating anti-inflammatory M2 macrophages. Furthermore, data also indicates a role of the AMPK pathway in XN-mediated anti-obesity effects.

## Table of Contents

Acknowledgements.....	iii
Abstract.....	iv
List of Figures.....	viii
Abbreviations.....	x
Chapter One: Literature Review.....	1
1.1 Epidemiology of Obesity.....	2
1.2 The Morphology and Physiology of Adipose Tissue.....	3
1.3 Immunometabolism.....	9
1.4 Current Treatments for Obesity.....	12
1.5 Phytochemicals: Are They The Safer Alternative?.....	13
1.6 AMPK as a Target for Metabolic Disorders.....	16
Chapter Two: Xanthohumol-induced Beiging of 3T3-L1 Mature Adipocytes: Role of AMPK Signaling Pathway.....	19
Abstract.....	20
2.1 Introduction.....	22
2.2 Specific Aims.....	24
2.3 Materials and Methods.....	26
2.4 Results.....	30
2.5 Discussion.....	33
2.6 Figures.....	36
Chapter Three: Xanthohumol Mediated Polarization of RAW264.7 Macrophages is Partly Mediated through the AMPK Signaling Pathway.....	46
Abstract.....	47
4.1 Introduction.....	49
4.2 Specific Aims.....	50
4.3 Materials and Methods.....	53
4.4 Results.....	55
4.5 Discussion.....	57
Samuels.....	vi

4.6 Figures .....	61
Chapter Four: Direct and Indirect Effects of Xanthohumol on the Induction of Beiging in 3T3-L1 adipocytes .....	68
6.1 Introduction .....	69
6.2 Specific Aim.....	70
4.3 Materials and Methods .....	72
6.4 Results .....	75
6.5 Discussion .....	76
6.6 Figures .....	78
Chapter Five: Conclusions .....	82
References .....	86



## List of Figures

Figure 1:	Targeting the adipocyte life cycle for prevention and treatment of obesity.	6
Figure 2:	Cross-talk between adipocytes and immune cells in adipose tissue.	11
Figure 3:	Chemical structure of xanthohumol.	15
Figure 4:	Proposed pathway for xanthohumol-induced adipocyte beiging via the AMPK signaling pathway.	18
Figure 5:	Working model for xanthohumol-induced beiging of white adipose tissue.	24
Figure 6:	Xanthohumol did not induce cytotoxicity in 3T3-L1 adipocytes.	35
Figure 7:	Xanthohumol treatment induces expression of brown/beige fat markers.	36
Figure 8:	Xanthohumol increases mitochondrial content in 3T3-L1 mature adipocytes.	37
Figure 9:	Xanthohumol increases the expression of PGC-1 $\alpha$ , a regulator of mitochondrial metabolism.	38
Figure 10:	Xanthohumol treatment induces UCP1 expression.	39
Figure 11:	Xanthohumol inhibits preadipocyte differentiation and adipogenesis.	40
Figure 12:	Effect of xanthohumol, dorsomorphin, and AICAR on AMPK activation.	41
Figure 13:	XN-mediated upregulation of UCP1 is decreased in the presence of AMPK inhibitor, dorsomorphin.	42
Figure 14:	XN-induced inhibition of adipogenesis is reversed in the presence of AMPK inhibitor, dorsomorphin.	43
Figure 15:	Dorsomorphin reversed the XN-induced decrease in lipid content in mature 3T3-L1 adipocytes.	44
Figure 16:	Working model for XN-mediated polarization of macrophages.	59
Figure 17:	Effect of XN on RAW264.7 cellular viability.	59
Figure 18:	Effect of XN on arginase-1 protein expression levels.	60

Figure 19:	Xanthohumol induces catecholamine secretion in RAW264.7 cells.	61
Figure 20:	Effect of xanthohumol on IL-10 secretion in RAW264.7 cells.	62
Figure 21:	Xanthohumol prevents M1 polarization in RAW264.7 cells.	63
Figure 22:	Effect of xanthohumol on p-AMPK protein expression.	64
Figure 23:	Effect of xanthohumol and AICAR on arginase-1 expression.	65
Figure 24:	Working model demonstrating the direct and indirect effects of XN on the induction of beige in WAT.	69
Figure 25:	Illustration of transwell co-culture system.	71
Figure 26:	Xanthohumol-stimulated RAW264.7 cells indirectly beige 3T3-L1 adipocytes.	76
Figure 27:	Mitochondrial content in mature 3T3-L1 adipocytes co-cultured with xanthohumol stimulated RAW264.7 macrophages.	77
Figure 28:	Catecholamine secretion levels in xanthohumol treated macrophages co-cultured with 3T3-L1 adipocytes.	78
Figure 29:	Effect of xanthohumol treated macrophages co-cultured with 3T3-L1 adipocytes on IL-10 secretion levels.	79

## Abbreviations

AICAR	5-aminoimidazole-4-carboxamide ribonucleotide
AMPK	Adenosine monophosphate-activated protein kinase
Arg-1	Arginase-1
BAT	Brown adipose tissue
BeAT	Beige adipose tissue
BMI	Body mass index
cAMP	Cyclic adenosine monophosphate
CS	Calf serum
CIDE-A	Cell death-inducing DFFA-like effector a
DEXA	dexamethasone
DMI	Differentiation media I
DMII	Differentiation media II
DMSO	dimethylsulfoxide
Dorso	Dorsomorphin
FBS	Fetal bovine serum
IBMX	isobutylmethylxanthine
IL-4	Interleukin 4
IL-10	Interleukin 10
INFY- $\gamma$	Interferon gamma
iNOS	Inducible nitric oxide synthase
Ins	Insulin
Iso	isoproterenol
LPS	lipopolysaccharide
p-AMPK	Phosphorylated AMPK
PGC-1 $\alpha$	Peroxisome proliferator-activated receptor $\gamma$ coactivator 1 $\alpha$
PPAR- $\gamma$	Peroxisome proliferator-activated receptor $\gamma$
PRDM16	PRD1-BF1-RIZ1 homologous domain containing 16
Rosi	rosiglitazone
T <sub>3</sub>	Triiodothyronine
T <sub>4</sub>	Thyroxine
TBS	Tris buffered saline
TBS-T	Tris buffered saline plus 0.1% tween 20
TBX-1	T box protein 1
Th1	Type 1 T helper cells
Th2	Type 2 T helper cells
UCP1	Uncoupling protein 1
WAT	White adipose tissue
XN	Xanthohumol
ZIC1	Zinc finger protein 1

## **Chapter One:**

### **Literature Review**

## 1.1 Epidemiology of Obesity

The prevalence of obesity has doubled since 1980 and in 2014, approximately 13% of the population 18 years and older globally were considered obese [5]. It has been projected that by 2030, 51.1% of the United States adult population will be obese [6]. Obesity is a chronic disease that causes and exacerbates other co-morbid diseases [7] and is the leading cause of mortality in the U.S. and worldwide [8]. These comorbidities include cardiovascular diseases, insulin resistance, gallbladder disease, musculoskeletal disorders, asthma, malignancies, mental health illnesses, and a decrease in the quality of life of an obese person [8]. Though preventable, obesity poses a major threat to the health of billions of lives worldwide.

The Body Mass Index (BMI) is an indirect measurement of a person's body fat, based on their weight and height, and assesses obesity in adults. In adults, a BMI greater than 30 indicates obesity. A BMI of 40 and greater indicates morbid obesity. At the forefront of concern, obesity is not limited to adults. In 2014, 41 million children, younger than 5 years old, were overweight or obese [5].

The etiology of obesity is complex and cannot be contributed to a single factor. Some factors that have been attributed to obesity include the adaptation of a sedentary lifestyle, an increase in readily available calorie-dense foods, genetic predispositions, existing hormonal conditions, medications, and socioeconomic status [9]. This makes obesity difficult to treat and prevent.

## **1.2 The Morphology and Physiology of Adipose Tissue**

Adipose tissue functions as a metabolic and endocrine organ responsible for maintaining systemic energy homeostasis as well as the production and secretion of various adipokines. These adipokines act to regulate food intake, energy metabolism, and inflammatory responses influencing the brain, muscle, liver, and other vascular tissues via autocrine, endocrine, and paracrine pathways [10]. Energy homeostasis is achieved when energy intake in the form of food, is equal to the amount of energy expenditure. Whenever energy intake exceeds energy expenditure, that excess energy is stored in the form of triglycerides in adipocytes which can eventually lead to obesity. Weight loss occurs when energy intake is significantly lower than the amount of energy expenditure. There are two types of obesity: hyperplastic, characterized by an increased number of adipocytes, and hypertrophic, characterized by an increase in the size of adipocytes. Adipose tissue is a heterogeneous, areolar connective tissue consisting of preadipocytes, adipocytes, multipotent stem cells, and immune cells such as macrophages [11].

### ***1.2.1 Adipogenesis***

Preadipocytes can be differentiated into mature adipocytes and mature adipocytes can be de-differentiated into preadipocytes, only to grow and re-differentiate into mature adipocytes again. This suggests that adipocytes can undergo cell turnover [11].

Adipocytes become mature and active through a process known as adipogenesis.

Adipogenesis is defined as the differentiation of a fibroblast-like preadipocyte into a mature lipid-laden, insulin-sensitive adipocyte [12]. *In vitro* studies, primarily using mouse 3T3-L1 cell models, have described adipogenesis as occurring in six stages. These

stages include mesenchymal precursors, committed preadipocyte, growth-arrested preadipocyte, mitotic clonal expansion, terminal differentiation, and mature adipocyte [13]. The stage of mesenchymal precursor is characterized by proliferation and the ability to commit to different lineages. The committed preadipocyte phase is characterized by the proliferation of preadipocytes, the commitment to differentiation, and adapting a fibroblast-like morphology.

Once grown to confluency, preadipocytes will arrest at the G<sub>0</sub>-to-G<sub>1</sub> cell cycle transition due to the contact inhibition. During the mitotic clonal expansion stage (MCE), preadipocytes will reenter the cell cycle, stimulated by hormones such as insulin (Ins), dexamethasone (Dexa), and isobutylmethylxanthine (IBMX). MCE involves several cycles of cell division and literature has suggested that differentiation requires this external stimuli [14]. Terminal differentiation involves cell cycle arrest, the induction of several transcription factors for adipogenesis like peroxisome proliferator-activated receptor gamma (PPAR- $\gamma$ ), and transcriptional activation of adipocyte-specific genes. The final stage of adipogenesis is the mature adipocyte where the adipocyte forms a large lipid droplet, PPAR- $\gamma$  becomes transcriptionally active, and adipocyte-specific genes are expressed [13]. This process of maturing preadipocytes can take 8 to 14 days.

The adipocyte life cycle makes for an attractive target pathway for treating obesity for example, one can induce apoptosis of preadipocytes, maturing preadipocytes, and the apoptosis of mature adipocytes. Scientists have also targeted the maturation of preadipocytes phase to inhibit adipogenesis and the stimulation of lipolysis of mature adipocytes. The molecular and biological processes that occur during adipogenesis remain unclear. Another approach towards anti-obesity therapy is to focus on the

Samuels

transdifferentiation of white adipose tissue to beige adipose tissue to increase energy expenditure in the form of heat.



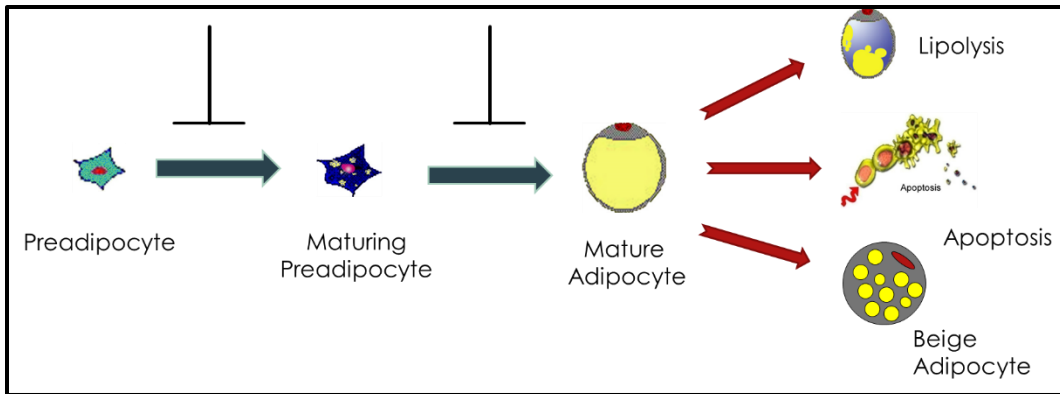


**Figure 1. Targeting the adipocyte life cycle for prevention and treatment of obesity [12].**

### ***1.2.2 White Adipose Tissue versus Brown Adipose Tissue***

There are two types of adipose tissue categorized by their antagonistic functions: white adipose tissue (WAT) stores excessive energy as triglycerides and brown adipose tissue (BAT) releases excessive energy in the form of heat. WAT is localized in humans subcutaneously and in the viscera. While classic BAT is thought to be present only in newborns, adults have BAT-like beige adipose tissue (BeAT) distributed throughout the axillary, paravertebral, mediastinal, upper abdominal regions, supraclavicular, and cervical areas [15].

White adipocytes can be distinguished from brown adipocytes by a large lipid droplet that predominates the cell and elongated mitochondria located within the thin cytoplasm. Brown adipocytes have smaller lipid droplets than white adipocytes. BAT contains an abundance of mitochondria that are large, spherical, and packed with laminar cristae. BAT also demands more vascular supply than that of WAT functioning for effective thermogenesis. The mitochondrial density and high vascularization of BAT is what gives the tissue its brown color [15].

It was once thought that brown and white adipocytes originate from the same mesenchymal progenitor cell, until recently, when scientists demonstrated that brown adipocytes arise from *Myf5* muscle-like progenitor cells [16]. Brown adipocytes express specific markers like UCP1, PGC-1 $\alpha$ , and PRDM16.

White adipocytes express specific proteins such as leptin and adiponectin. Leptin, the ob protein produced in WAT, expression levels are directly proportional to white fat mass and show a strong relationship with the size of adipocytes. The increase in

secretions and expression levels of leptin from adipocytes upregulates anabolic processes. Activation of  $\beta$ -adrenergic receptors and increases in the intracellular cyclic AMP (cAMP) levels inhibit leptin expression, in other words, catabolic processes are inhibited [17]. The differences between BAT and WAT contribute to their antagonistic roles in energy metabolism and homeostasis.

### ***1.2.3 Thermogenic Properties of BAT***

The abundance of mitochondria found in BAT contain respiratory chains that allow these cells to oxidize substrates at a high rate. The dissipation of heat produced from fatty acid oxidation makes BAT thermogenesis possible. In response to stress, like cold air or excessive energy, a mammal's sympathetic nervous system will be activated and norepinephrine will be released. Norepinephrine then interacts with  $\beta$ -adrenergic receptors located on the plasma membrane of a brown adipocyte forming cAMP. cAMP is responsible for activating type 2 deiodinase, a catalyst that converts inactive thyroxine ( $T_4$ ) to the biologically active triiodothyronine ( $T_3$ ) in brown adipocytes.  $T_3$  serves to increase energy expenditure, increase mitochondrial functioning, and increase the basal metabolic rate of an individual. cAMP can also accelerate the amount of free fatty acids available to be used as fuel for thermogenesis and as an activator of UCP1 [18]. UCP1 uncouples respiration from ATP synthesis and in turn, large amounts of energy is released in the form of heat.

### ***1.2.4 Beiging of WAT: The New Brown Fat***

Recently, a third type of adipose tissue has been identified as beige adipose tissue (BeAT). These beige fat cells emerge from WAT as a result of the “browning/beiging” of mature adipocytes. Beige cells within white adipose depots do not share the same cellular lineage as classic brown adipocytes; instead, they arise from a non-Myf-5 cell lineage [2]. Research has demonstrated that UCP1 is not constitutively expressed in BeAT, like BAT, but that it is inducible and once induced, BeAT will exert its thermogenic functions.

WAT can be transdifferentiated into BeAT under  $\beta$ -adrenergic stimulation and cold exposure [19]. Since the amount of BAT in the human body decreases with age, and body weight increases [15], it is ideal to target the browning of WAT for obesity therapy.

### **1.3 Immunometabolism**

In the obese state, adipose tissues produce a significantly large amount of pro-inflammatory cytokines and adipokines secondary to its abundance of white adipocytes and pro-inflammatory immune cells such as ‘classically activated’ M1 macrophages. This is why obesity is associated with systemic, chronic, low-grade inflammation. In the lean state, ‘alternatively activated’ M2 macrophages are more abundant in WAT and secrete anti-inflammatory cytokines and catecholamines. M2 type macrophages have also been associated with maintaining insulin sensitivity. M1 macrophages comprise 10-15% of adipose tissue in lean states but in obese states, macrophages make up 40-50% of the stromal vascular cells in visceral adipose tissue [20].

Monocytes are precursors to macrophages and macrophages can undergo polarization in response to their microenvironment. In obesity, interferon- $\gamma$  (IFN- $\gamma$ ), and

lipopolysaccharide (LPS) polarize macrophages toward the M1 phenotype. M1 type macrophages secrete pro-inflammatory cytokines such as interleukin-6, tumor necrosis factor- $\alpha$ , and interleukin-12, as well as nitric oxide [20]. M1 macrophages are associated with killing responses [21].

The polarization of the M2 type macrophage is stimulated by interleukin-4 (IL-4). M2 type macrophages express arginase – 1, anti-inflammatory cytokines including, but not limited to, interleukin-10 (IL-10), interleukin-1 (IL-1) receptor antagonists, and catecholamines. Arginase – 1 is an enzyme involved in the urea cycle where it functions to hydrolyze arginine to urea and ornithine, removing nitrogen from the body. Ornithine can generate proline which synthesizes collagen. This production of collagen, regulated by arginase – 1, is said to have wound healing and tissue repair effects [22]. Arginase – 1 is constitutively expressed in the liver but is inducible upon external stimulation and is regulated in macrophages. M2 macrophages can contribute to the browning of WAT but this mechanism is poorly understood [3].

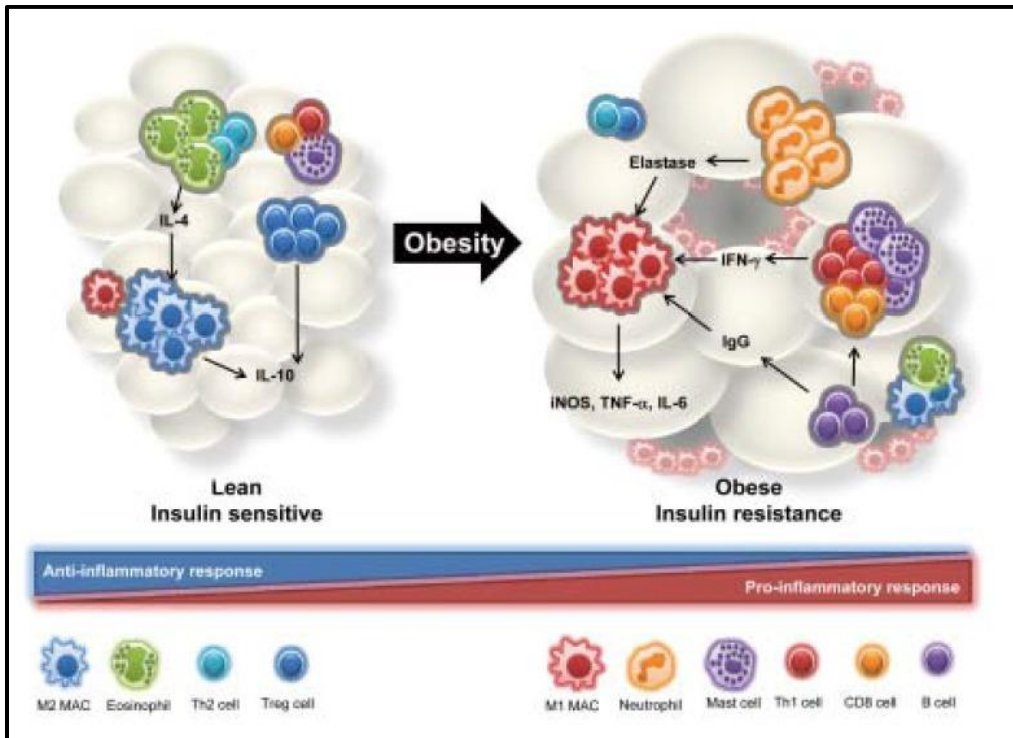


Figure 2. Cross-talk between adipocytes and immune cells in adipose tissue [20].

## 1.4 Current Treatments for Obesity

The standard recommendations for weight loss include increasing physical activity, decreasing caloric intake, changing dietary habits, and behavior modifications such as counseling or support groups. Bariatric surgery is also an option but it is high risk and expensive. Though these lifestyle changes can result in weight loss, they do not ameliorate the obesity epidemic.

Pharmacotherapeutics approved as anti-obesity drugs on the market today act in one of two ways: decreasing fat accumulation and acting centrally to suppress appetite. In the past, anti-obesity drugs have been removed from the market due to adverse effects including sibutramine and amphetamines. Amphetamine was a concoction of other drugs making it addictive, increasing the risk of myocardial infarction, and sudden death. Sibutramine, an amphetamine analog, was removed from the market after it was associated with an increased risk of heart attack and stroke [23].

The US Food and Drug Administration has recently approved several new weight loss drugs. Five new therapies include orlistat, lorcaserin, phentermine/topiramate, naltrexone/bupropion, and liraglutide [23]. Considering obesity is a global epidemic, the number of FDA approved medications to address this issue is limited. Additionally, the existing anti-obesity medications are accompanied with adverse side effects and do not directly target adipose tissue or energy expenditure, making these treatments less efficient.

## 1.5 Phytochemicals: Are They The Safer Alternative?

Natural health products have a long-standing reputation of serving as medications and healing therapies. Phytochemicals are characterized based on their structure and include polyphenols, alkaloids, and isoprenoids. There has been extensive research demonstrating that phytochemicals are anti-oxidants, anti-cancer agents, immune system activators, metabolism modulators, and more. Phytochemicals have also been evaluated for their efficacy in the treatment of obesity. Many phytochemicals such as guggulsterone, curcumin, and resveratrol inhibit adipogenesis, stimulate lipolysis in adipocytes, and even function as browning agents [12, 24, 25].

### 1.5.1 Xanthohumol

Xanthohumol is a prenylated flavonoid found in the hops flower, *Humulus lupulus*. Hops are used to preserve and add flavor to beer. XN has already been identified to have anti-cancer, anti-diabetic and anti-oxidant characteristics [4]. Dr. Rayalam's lab has previously reported that XN inhibits adipogenesis and increases lipolysis in 3T3-L1 adipocytes [25].

XN has been shown to possess anti-carcinogenic, anti-oxidant, and anti-diabetic properties [26-28]. It has been suggested that the chemical structure of XN is responsible for its wide range of biological activities. The XN molecule is comprised of two aromatic rings substituted with hydroxyl and methoxyl groups, and a prenyl unit (Fig. 3). Because of its prenyl and  $-OCH_3$  group, XN is highly lipophilic and has a strong affinity for biological membranes [29]. Hirata et al., reported that XN inhibits the cholesteryl ester



transfer protein (CETP), resulting in an increase in high density lipoprotein levels. This inhibitory effect can be attributed to XN's prenyl group and chalcone structure [30].

Costa et al., demonstrated that XN consumption in high-fat diet fed mice prevented weight gain, decreased blood glucose levels, triglyceride, and cholesterol levels, and improved insulin sensitivity. XN also activated the AMPK signaling pathway, suppressing lipogenesis [31]. Additionally, XN is suggested to be an agonist of the farnesoid X receptor through a selective bile acid receptor modulator, similar to the phytochemical guggulsterone. This interaction with FXR results in the amelioration of lipid and glucose metabolism [32]. XN increased the mRNA expression of TGR5, a G protein-coupled bile acid receptor, in mature 3T3-L1 adipocytes, indicative of its possible role in the TGR5 pathway [33]. Oral administration of XN improved inflammatory markers and the metabolic profile in diet-induced obese C57BL/6J mice [34]. However, XN's beiging effects on adipocytes and the underlying mechanisms remain to be understood.

In this study, we have shown that XN induces beiging of 3T3-L1 adipocytes both directly and indirectly, and these actions are dependent upon the activation of the AMPK pathway.

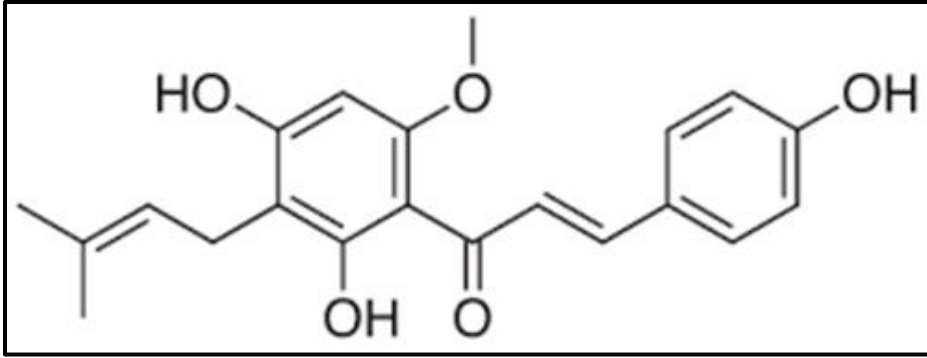


**Figure 3. Chemical structure of xanthohumol.**

## 1.6 AMPK as a Target for Metabolic Disorders

AMPK is a master metabolic switch and is believed to be expressed in a number of tissues including BAT. The thermogenic activities of BAT are activated by AMPK [35]. BAT activation is stimulated in response to cold conditions resulting in the phosphorylation of AMPK to its active form to begin to increase thermogenesis. AMPK is an enzyme complex composed of three subunits, the catalytic  $\alpha$  subunit and the two regulatory  $\beta$  and  $\gamma$  subunits. The  $\alpha 1$  isoform is the predominant isoform expressed in adipose tissue [36]. AMPK is phosphorylated at Thr172 of the  $\alpha$  subunit and as a result, becomes biological active [37].

In our metabolic organs that function to maintain energy homeostasis, like adipose tissue, phosphorylated-AMPK (p-AMPK) inhibits anabolic processes and upregulates catabolic processes. p-AMPK works to enhance fatty acid oxidation by the phosphorylation of acetyl-CoA carboxylase, thereby increasing the incidence of fatty acid degradation [37]. AMPK's role in adipose tissue metabolism has been characterized [38] but it remains unclear whether AMPK is involved in the being of white adipocytes.

Provided the importance of AMPK in modulating energy homeostasis, little is known about the physiological roles of AMPK in brown and white adipose tissue, or the regulation of AMPK in these tissues. Understanding AMPK's role in regulating BAT metabolism is attractive because of BAT's unique ability to release excess energy in the form of heat via uncoupled metabolism.

Recent studies propose that AMPK influences adipocyte functioning and the inflammatory environment of adipose tissues [39, 40]. Chronic nutrient overload creates

stress in adipose tissue. This stress results in the accumulation of lipids in adipocytes in addition to the storage of fat in the liver, muscles, and pancreas. Consequently, this stimulates the innate immunity defense where pro-inflammatory cytokines are released and monocytes are recruited into adipose tissue[41].

An increase in pro-inflammatory macrophage content of adipose tissue increases adiposity [42]. Activated AMPK has been suggested to suppress the pro-inflammatory environment and promote M2 macrophage polarization within adipose tissue [43]. Since obesity is characterized by chronic, low-grade inflammation, activating AMPK in adipose tissue may be found to be beneficial in improving the metabolic profile in obese states.

In the current study, we aimed to elucidate the role of XN in brown-like adipocyte formation in 3T3-L1 adipocytes and to investigate the possible molecular mechanism underlying this process. It was also our goal to define XN-mediated polarization of macrophages and AMPK's role in this process.

Our data demonstrates that XN induces the beiging of adipocytes and polarizes macrophages toward the anti-inflammatory phenotype. These multi-faceted anti-obesity effects of XN are mediated via the AMPK signaling pathway.

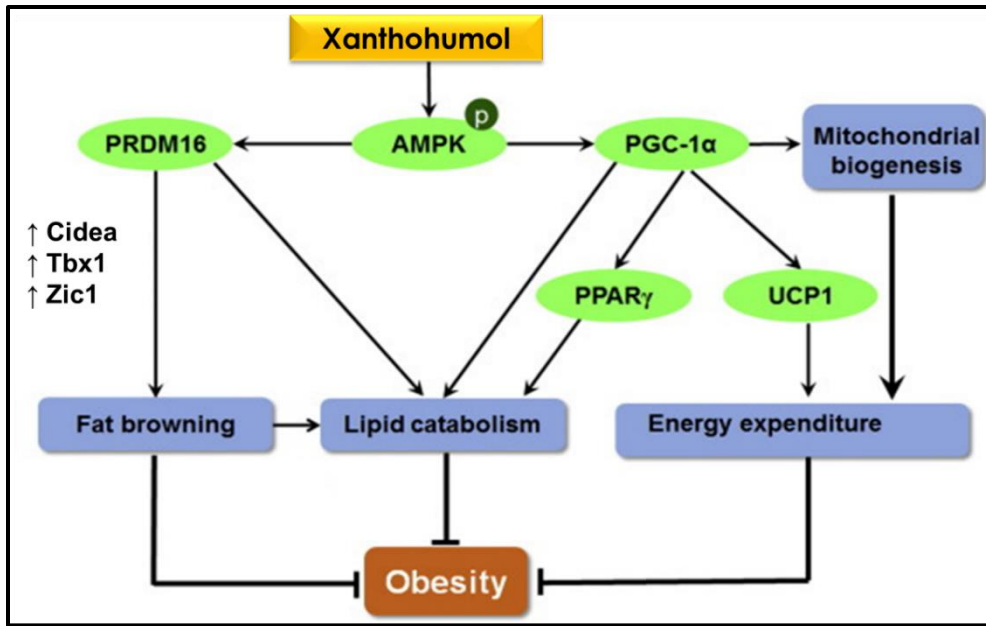


**Figure 4.** Proposed pathway for xanthohumol-induced adipocyte browning via the AMPK signaling pathway: (→) stimulatory, (⊥) inhibitory, (↑) upregulation.

## **Chapter Two**

### **Xanthohumol-induced Beiging of 3T3-L1 Mature Adipocytes: Role of AMPK Signaling Pathway**

## Abstract

Xanthohumol (XN), a flavonoid compound extracted from the hop plant *Humulus lupulus*, has been studied for its anti-cancer and anti-adipogenic effects. In this study, we have investigated the effects of XN on the inhibition of adipogenesis and the induction of browning in 3T3-L1 adipocytes. Furthermore, we provide evidence, for the first time, on the role of the adenosine monophosphate-activated protein kinase (AMPK) signaling pathway in XN-induced anti-obesity effects.

Browning of white adipose tissue, WAT, is emerging as a novel approach to address obesity. AMPK is activated in response to stress-like exposure to cold and has been shown to induce browning of WAT. Treatment of 3T3-L1 adipocytes with XN decreased lipid content during adipogenesis and increased the expression of uncoupling protein 1 (UCP1), in a dose-dependent manner in mature adipocytes. XN further increased mitochondrial activity in mature adipocytes after 24 hours, suggesting browning of adipocytes.

To demonstrate the role of AMPK pathway in XN-induced anti-obesity effects, mature adipocytes were treated with either 0.1% DMSO or XN 25 $\mu$ M in the presence or absence of dorsomorphin, an established inhibitor of the AMPK pathway, and 5-Aminoimidazole-4-carboxamide ribonucleotide (AICAR), an AMPK stimulator. XN increased the expression of phospho-AMPK (p-AMPK) and this XN-induced increase in AMPK activation was diminished in the presence of dorsomorphin. On the other hand, co-incubation of XN plus AICAR demonstrated an additive effect on the activation of AMPK. Likewise, dorsomorphin reversed XN-induced inhibition of adipogenesis while

XN plus AICAR demonstrated an additive effect on the inhibition of lipid content during adipogenesis. Additionally, XN promoted lipolysis of mature 3T3-L1 adipocytes but this effect was also reversed in the presence of dorsomorphin. These results provide evidence for the potential role of AMPK pathway in XN-induced anti-obesity effects in 3T3-L1 adipocytes.



## 2.1 Introduction

Until recently, adipose tissue has been identified to function as a metabolic and endocrine organ, having both positive and negative characteristics. Excessive accumulation of adipose tissue leads to obesity, a chronic metabolic disease characterized by chronic, low-grade inflammation. Obesity increases the risk of developing hypertension, certain cancers, cardiovascular disease, musculoskeletal disorders, insulin resistance, as well as several other co-morbidities [10].

At the onset of obesity, adipocytes become hypertrophic and hyperplastic. WAT is comprised of mature, lipid laden adipocytes, immune cells such as macrophages, preadipocytes, and stromal vascular cells. WAT lack mitochondria and UCP1, and thus thermogenic properties, unlike BAT. Thermogenesis has been shown to decrease adiposity and diabetes in both mice and adult humans [44-47]. An intermediate type of adipocyte is the “beige” or “brite” adipocyte. This cell type is functionally and morphologically similar to the brown adipocyte but is derived from white adipocytes via transdifferentiation or a process known as “beiging” in response to cold exposure or beta-adrenergic stimuli [48].

Phytochemicals have been recently proposed to act as beiging agents and are gaining the attention of scientists. Several phytochemicals such as resveratrol, curcumin, quercetin, and genistein have been demonstrated to be promising BAT activators or serve to increase thermogenesis therefore, treating obesity and the metabolic syndrome [49]. Literature has suggested that XN, a prenylated flavonoid found in hops and beer itself, induces apoptosis of mature adipocytes and inhibits adipogenesis in the mouse 3T3-L1

adipocyte cell line [50]. To the contrary, Mendes and colleagues claimed that XN does not improve the metabolic profile linked to obesity [51]. Therefore, we sought to explore XN's potential anti-obesity effects *in vitro*.

As a complex, multi-factorial, chronic disease, obesity develops from an imbalance of energy homeostasis. Consequently, adipocytes grow and expand. These processes are dependent on the regulation of adipogenesis. Furthermore, hyperplastic adipocytes also negatively impact the pathogenesis of obesity. Anti-obesity therapies that target the adipocyte life cycle or mature adipocytes call for an ideal tool in decreasing adiposity [12].

AMPK is an energy gauge that, once activated, promotes catabolic pathways and inhibits anabolic pathways that consume ATP. Several studies have implicated the AMPK enzyme as a potential signaling target for obesity therapy [52, 53].

AMPK can be activated by pharmacological interventions such as AICAR, metformin, phytochemicals, and hormones like adiponectin, catecholamines or the cytokine interleukin 6 [52, 54, 55]. AMPK has also been noted to be inhibited by dorsomorphin, a competitive ATP cell permeable pyrazolopyrimidine derivative [56].

Whether XN can activate AMPK and if AMPK signaling has a role in XN's anti-obesity effects remains to be defined. We hypothesize that the effects of XN in the beiging of white adipocytes is partly mediated by the activation of the AMPK signaling pathway.

## **2.2 Specific Aims**

XN's ability to inhibit adipogenesis, induce lipolysis, lower blood glucose and triglyceride levels, has been reported, however, XN's effects on BAT activity or beiging of WAT has not been investigated. *In this study, we have two specific aims (Figure 5).*

*Specific aim 1: To demonstrate the beiging effects of XN using 3T3-L1 adipocytes.*

*Specific aim 2: To investigate AMPK's possible role in XN-mediated beiging.*

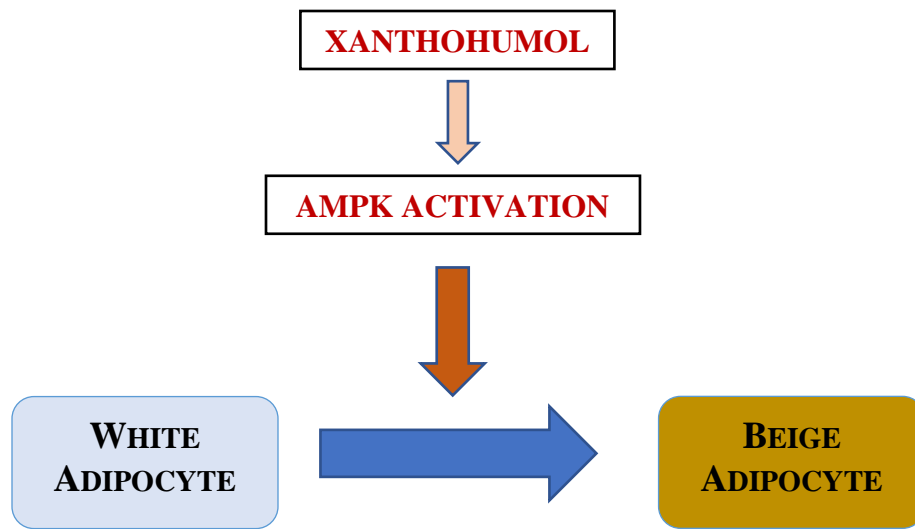


**Figure 5. Working model for xanthohumol-induced beiging of white adipose tissue.**

## **2.3 Materials and Methods**

### ***2.3.1 Cell culture and differentiation***

Dulbecco's Modification of Eagle's Medium (DMEM; Corning, Manassas, VA, USA) supplemented with 10% calf serum (CS; Invitrogen, Grand Island, NY, USA) and 1% penicillin streptomycin (PS; Sigma-Aldrich, St. Louis, MO, USA) was used to culture 3T3-L1 mouse embryo preadipocytes (Zenbio) at 37°C in a 5% CO<sub>2</sub> incubator.

Once confluent, cells were maintained in differentiation induction medium I (DMI) comprised of 1 mg/ml of insulin (Ins; Sigma-Aldrich, St. Louis, MO, USA), 5 µM of dexamethasone (Dexa; Sigma-Aldrich, St. Louis, MO, USA), 0.5 mM of isobutylmethylxanthine (IBMX; Sigma-Aldrich, St. Louis, MO, USA), and 1 µM of rosiglitazone (Rosi; Sigma-Aldrich, St. Louis, MO, USA) for three days in DMEM plus 10% fetal bovine serum (FBS; Invitrogen, Grand Island, NY, USA) and 1% PS. Following DMI, cells were then maintained in differentiation medium II (DMII) containing 10% FBS, 1% PS, 1 mg/ml of Ins, and 1 µM of Dexa. Unless otherwise stated, cells were maintained in DMII for 8-10 days before treatment and analysis and until cells matured with a minimum of 90% lipid droplet accumulation. Maintenance medium was changed every other day. XN 6.25 µM and XN 25 µM were the two optimal doses used in this study based on cell viability assays.

### ***2.3.2 Cytotoxicity***

Mature 3T3-L1 adipocytes were treated with 0.1% dimethylsulfoxide (DMSO; Sigma-Aldrich, St. Louis, MO, USA) vehicle control or XN for 24 hours. Cell viability was measured using Prestoblu<sup>TM</sup> Cell Viability Reagent (ThermoFisher Scientific,

Grand Island, NY, USA) according to the manufacturer's protocol. The absorbance of metabolically active cells was quantified 1 hour after incubation in the reagent using the Biotek Synergy HT (Winooski, VT, USA) microplate reader at 570nm.

### **2.3.3 Immunoblot analysis**

Proteins were lysed and extracted from mature 3T3-L1 adipocytes after treatment with 0.1% DMSO, XN 6.25-25  $\mu$ M (XN; Tocris Bioscience, Bristol, UK), isoproterenol 10  $\mu$ M (Iso; Sigma-Aldrich, St. Louis, MO, USA), dorsomorphin 10  $\mu$ M (Dorso; Abcam, Cambridge, MA), or 5-Aminoimidazole-4-carboxamide ribonucleotide 2 mM (AICAR; Abcam, Cambridge, MA, USA) for 24 hours using ice cold RIPA Lysis and Extraction buffer complete with protease and phosphatase inhibitors (ThermoFisher Scientific, Grand Island, NY, USA).

Whole cell lysate was then prepared by centrifuging cells for 10 minutes at 13,300g at 4°C. Following protein estimation, as determined by the Pierce BCA Protein Assay Kit (ThermoFisher Scientific, Grand Island, NY, USA), the proteins were diluted in 4X sample buffer and heated for 5 minutes at 95°C.

After reducing and denaturing, proteins were loaded and separated on 4-20% SDS polyacrylamide gels and transferred to a polyvinylidene difluoride (PVDF) membrane using the Trans-blot Turbo system (Bio-Rad, Hercules, California, USA). The membranes were then blocked in Tris buffered saline plus 0.1% Tween 20 (TBS-T) containing 3-5% BSA blocking buffer for 1 hour at room temperature and then incubated in primary antibodies in TBS-T containing 3-5% BSA blocking buffer for 1 hour at room temperature.

The primary antibodies used in this study included: anti-UCP1, anti-CIDE-A, anti-TBX-1, anti-phospho-AMPK (Thr172), (all from Abcam, Cambridge, MA, USA), anti-PGC-1 $\alpha$ , anti-ZIC1, mouse anti- $\alpha$ -tubulin (Novus Biologicals, Littleton, CO, USA), and mouse anti- $\beta$ -actin (Santa Cruz Biotechnology, Cambridge, MA, USA).

Following primary antibody incubation, the membranes were then washed three consecutive times with TBS-T and incubated with LiCor secondary antibodies (LiCor Biosciences, Lincoln, NE, USA) for 45 minutes at room temperature. The membranes were rinsed another three times, consecutively, with TBS-T, and fluorescent imaging was developed using the LiCor Odessey CLX imaging system (LiCor Biosciences, Lincoln, NE, USA). Relative protein levels were quantified using Image Studio Ver. 5.2 (LiCor Biosciences, Lincoln, NE, USA).

#### ***2.3.4 Mitochondrial biogenesis***

Mature 3T3-L1 adipocytes were treated with 0.1% DMSO, XN 6.25  $\mu$ M, XN 12.5  $\mu$ M, XN 25  $\mu$ M, and Iso 10  $\mu$ M for 24 hours and incubated with Mitotracker® Green FM (Invitrogen, Grand Island, NY, USA) as per the manufacturer's instructions.

Mitochondrial activity was measured using the Biotek Synergy HT (Winooski, VT, USA) microplate reader at 516nm and images were captured using the EVOS FL Auto Imaging System (ThermoFisher Scientific, Grand Island, NY, USA) microscope.

### ***2.3.5 Oil Red O staining***

DMSO and XN treated cells were matured for 4-8 days, followed by washing with phosphate buffered saline (PBS), fixation with 10% formalin for 1 hour at room temperature, and washing again three times with deionized water. A 6:4 mixture of Oil Red O solution (0.6% Oil Red O dye in isopropanol) and water was added to the cells for 20 minutes followed by a wash four times with deionized water. Finally, hematoxylin was layered over the cells and incubated for one minute, then rinsed. Lipid droplets were imaged under phase contrast using the EVOS FL Auto Imaging System (ThermoFisher Scientific, Grand Island, NY, USA) microscope.

### ***2.3.6 AdipoRed™ Adipogenesis Assay***

Preadipocytes treated with 0.1% DMSO, XN 25  $\mu$ M, Dorso 10  $\mu$ M or AICAR 2 mM on day 0 were treated every other day until day 8 of the adipocyte life cycle. Lipid accumulation was quantified using the AdipoRed™ assay (Lonza, USA) per the manufacturer's protocol. Mature adipocytes treated with 0.1% DMSO, XN 25  $\mu$ M, Dorso 10  $\mu$ M, or AICAR 2 mM were also assayed on day 8 for lipid quantification. Lipid quantification was obtained using the Biotek Synergy HT (Winooski, VT, USA) microplate reader at a fluorescence of 485/590 nm.



### **2.3.7 Statistical analysis**

All data were expressed as the mean  $\pm$  SEM, minimum n = 3. Comparisons were made by using one-way analysis of variance (ANOVA) on GraphPad Prism software, followed by Tukey's post hoc tests. Statistical significance was reported as P < 0.05, P 0.01, P < 0.001 or P < 0.0001.

## **2.4 Results**

### ***2.4.1 XN does not produce cytotoxic effects in 3T3-L1 adipocytes***

Mature 3T3-L1 adipocytes were treated with 0.1% DMSO, XN 25 $\mu$ M and XN 50  $\mu$ M for 24 hours. Following incubation for 24 hours, XN was not significantly cytotoxic to adipocytes at the indicated doses (Fig. 6).

### ***2.4.2 XN induces beiging of mature 3T3-L1 adipocytes***

To investigate the beiging effect of XN, 3T3-L1 adipocytes were used as a cellular model and stimulated with XN 6.25-25  $\mu$ M and isoproterenol 10  $\mu$ M as a positive control. XN 25  $\mu$ M significantly increased the expression of beige/brown markers CIDE-A, ZIC1, and TBX-1 (Fig. 7).

### ***2.4.3 XN increases thermogenic marker expression and induces mitochondrial biogenesis in adipocytes***

To determine if XN increases mitochondrial biogenesis, a characteristic of browning, MitoTracker® Green FM was performed that specifically binds to mitochondria. As shown in Fig. 8, mitochondrial content was markedly elevated in XN-treated groups and this was further confirmed by Western Blot analysis of PGC-1 $\alpha$ , a central driver of mitochondrial biogenesis in adipocytes (Fig. 9). Furthermore, increased expression of mitochondrial uncoupling protein 1 (UCP1) (Fig.10), a thermogenic marker, support these findings and suggests further XN-induced beiging of mature 3T3-L1 adipocytes.

#### ***2.4.4 XN regulates lipid metabolism in 3T3-L1 adipocytes***

To establish XN's multifaceted anti-obesity effects on 3T3-L1 adipocytes, we examined whether XN promotes lipolysis and inhibits preadipocyte differentiation. Preadipocytes were treated with XN 6.25-25  $\mu$ M and 0.1% DMSO vehicle control on day 0 until day 8 of differentiation. As visualized by Oil Red O staining (Fig. 11), XN decreased the number and size of lipid droplets suggesting that XN inhibits adipogenesis and suppresses lipid accumulation.

#### ***2.4.5 XN stimulates the phosphorylation of AMPK in mature 3T3-L1 adipocytes***

AMPK is an important regulator of metabolic homeostasis within a cell [57, 58]. A consequence of the activation of AMPK signaling is lipid metabolism modulation, mitochondrial biogenesis, and a decrease in blood glucose levels [58]. Therefore, we sought to investigate the effect of XN on AMPK phosphorylation. XN treatment of

mature 3T3-L1 adipocytes for one hour, significantly enhanced the expression levels of p-AMPK, similar to that of the AMPK agonist AICAR (Fig. 12).

#### ***2.4.6 AMPK inhibition eliminates the thermogenic effects of XN on 3T3-L1 adipocytes***

To identify the possible mechanism underlying the beiging effect of XN, the selective AMPK inhibitor, dorsomorphin, was used to determine UCP1 protein expression levels. When mature 3T3-L1 adipocytes were treated with XN 25  $\mu$ M for one hour, results showed an increase in UCP1 expression. However, this effect was reversed by co-incubation of dorsomorphin with XN, suggesting that XN-induced beiging is mediated via AMPK signaling pathway (Fig 13).

#### ***2.4.7 XN regulates adipogenesis through the AMPK pathway***

Literature suggests that AMPK is crucial for the mediation of preadipocyte maturation [59]. We demonstrated that XN inhibits adipogenesis in 3T3-L1 cells but this inhibition is ameliorated in the presence of dorsomorphin (Fig. 14). Thus, XN-induced inhibition of adipogenesis is regulated through the AMPK pathway.

#### ***2.4.7 XN stimulation of lipolysis is mediated through the AMPK pathway***

Differentiated, mature adipocytes were exposed to XN, AICAR, and dorsomorphin for 72 hours. Fig. 15 shows the effects of these compounds on the induction of lipolysis in 3T3-L1 cells. AdipoRed assay results showed that XN decreased lipid content by  $49\% \pm 6$  when compared to the control. AICAR treatment alone

decreased lipid content by  $8\% \pm 22$  when compared to the control. To the contrary, XN in the presence of AICAR decreased lipid droplet size and content by  $51\% \pm 7$ .

Dorsomorphin increased lipid content significantly, by  $61.5\% \pm 4.29$ . XN's stimulation of lipolysis was abolished in the presence of dorsomorphin.

## **2.5 Discussion**

Obesity remains to be an epidemic worldwide and is a risk factor for several co-morbidities. Current therapies targeting obesity are limited and are accompanied by unwanted side effects. Therapies that focus on BAT or BeAT activation make for an attractive target for the treatment of obesity and the metabolic syndrome [60]. In the present study, we have demonstrated that XN induces the brown fat-like phenotype from mature white adipocytes and drives thermogenesis through a dose-dependent elevated expression of brown fat markers such as UCP1, CIDE-A, ZIC1, and PGC-1 $\alpha$ . Wu et al., suggested that TBX-1 is a beige fat specific marker and XN significantly upregulated the expression of TBX-1 indicating XN's role in the induction of beiging white adipocytes [2].

A key characteristic of brown fat and beige fat is increased numbers of mitochondria [61]. Our data suggests that XN significantly increases mitochondrial biogenesis in mature 3T3-L1 adipocytes accompanied by the upregulation of PGC-1 $\alpha$ , the central regulator of mitochondrial biogenesis and thermogenic programming [62]. In addition, UCP1 expression was elevated in 3T3-L1 adipocytes upon stimulation with XN, confirming mitochondrial oxidation and the acquisition of thermogenic properties [63].

XN appears to inhibit the differentiation of preadipocytes and decrease lipid accumulation [25, 51] in 3T3-L1 cells. Our data confirms that XN-treated adipocytes are subjected to lipolysis and suppressed lipogenesis.

Previous studies provide evidence that pharmacological and genetic approaches to activate AMPK improves the metabolic profile [64-66]. Therefore, activation of the AMPK signaling pathway is crucial to achieving and maintaining energy homeostasis [67]. Our data demonstrates that XN significantly upregulates the expression of p-AMPK, and this effect is ameliorated with the inhibition of p-AMPK. Flavonoids such as curcumin, chrysin, and quercetin induce the brown-like phenotype in 3T3-L1 adipocytes and this browning is mediated through the AMPK pathway [68]. To the contrary, it has been suggested that AMPK is activated but accompanied by constant levels of total AMPK during beiging of white adipocytes [36]. In this study, we have shown that the prenylated flavonoid, XN, significantly increased the expression of the thermogenic/brown fat marker protein UCP1, and this upregulation is mediated partly through the activation of the AMPK pathway as evidenced by the arrest of UCP1 expression with co-incubation of XN with dorsomorphin.

Literature has supported the notion that there exists several pathways responsible for the beiging of white adipocytes, including numerous kinases,  $\beta$ -adrenergic receptor activation, bone morphogenetic protein, thyroid hormones, and fibroblast growth factor 21 activation[52, 69]. To date, little is known about the extent of AMPK's involvement in XN-mediated beiging of 3T3-L1 cells. Therefore, future molecular mechanistic studies are warranted to support our findings.

The anti-adipogenic effects of flavonoids have been suggested to be regulated via the AMPK signaling pathway in 3T3-L1 adipocytes [70, 71], however, the role of AMPK in regulating lipolysis has been controversial. Yin et al., reported that AMPK activation is essential in promoting lipolysis *in vitro* [72] while *in vivo* data demonstrated that AMPK activation is anti-lipolytic [73]. To identify its role in the XN-induced lipolytic pathway, we treated mature adipocytes with AICAR or dorsomorphin. Our data shows that XN suppressed adipocyte differentiation and reduced the accumulation of lipid content and lipid droplet size. Noteworthy, this anti-adipogenic and lipolysis effect of XN was abolished in the presence of dorsomorphin.

Taken together, these results provide a novel insight into the molecular mechanism behind XN's multi-faceted anti-obesity effects. In conclusion, the XN-induced activation of AMPK results in the beiging of mature 3T3-L1 adipocytes, a downregulation of lipid content, and the inhibition of adipogenesis.

## 2.6 Figures

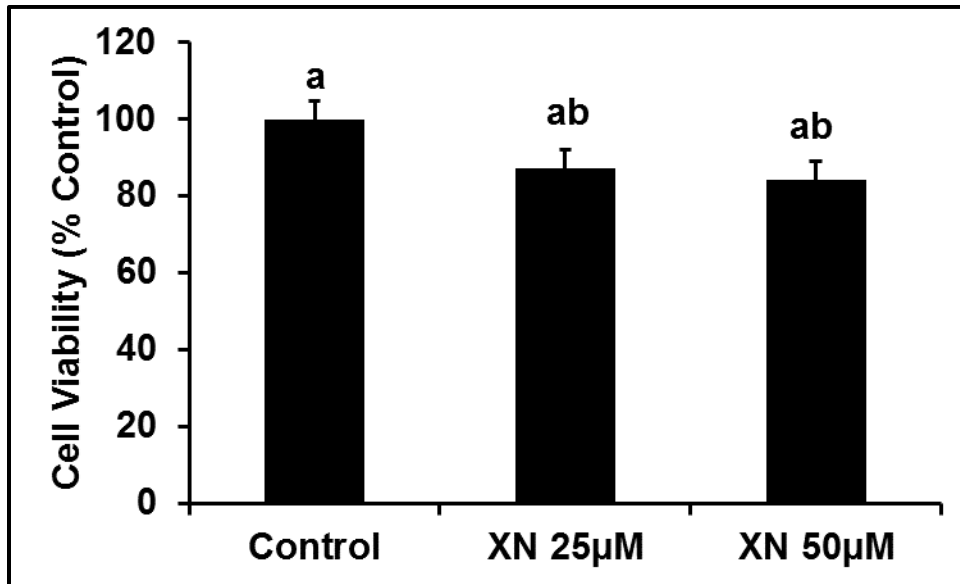


**Figure 6. XN did not induce cytotoxicity in 3T3-L1 adipocytes.** Mature 3T3-L1 adipocytes were treated with varying doses of XN for 24 hours, followed by measurement of cell viability using Prestoblu<sup>TM</sup> Cell Viability Reagent. All data are presented as mean  $\pm$  SEM. Differences between treatment groups were determined by one-way analysis of variance (ANOVA) using GraphPad Prism software, followed by Tukey's post hoc tests. Means denoted with different letters are statistically different  $P < 0.05$ .

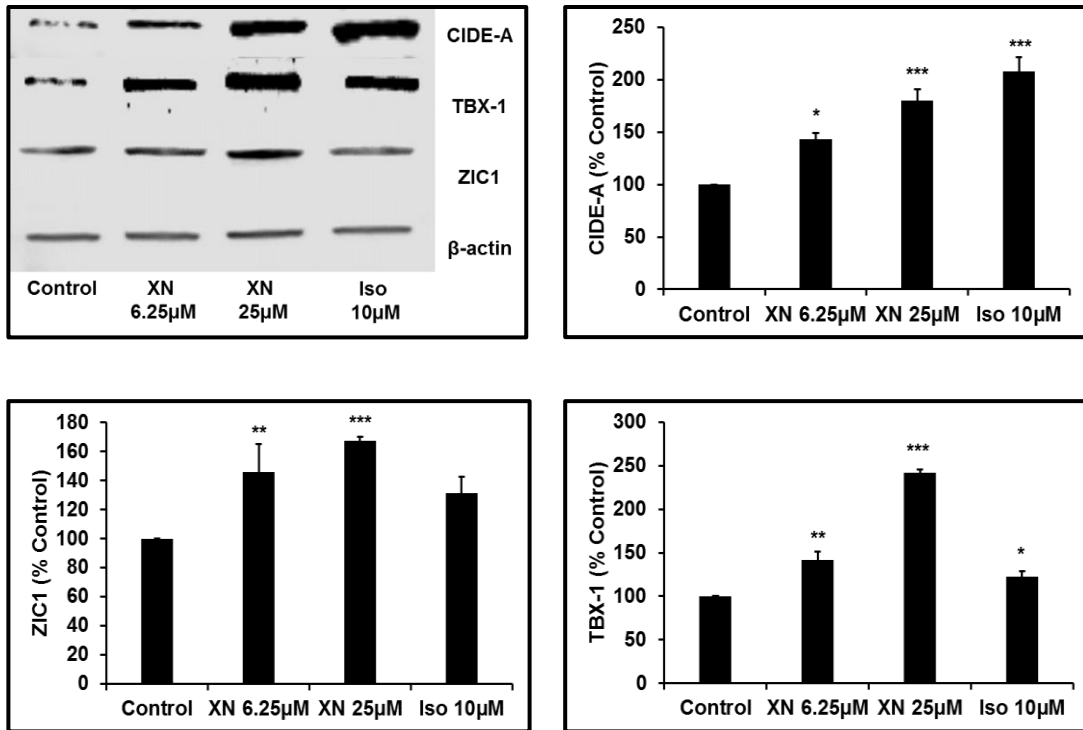


**Figure 7. XN treatment induces expression of brown/beige fat markers.** 3T3-L1 mature adipocytes were treated with varying XN concentrations for 24 hours and expression of CIDE-A, ZIC1, and TBX-1 were determined by western blotting and quantified by densitometry analysis. All data are presented as mean  $\pm$  SEM. Statistical significance between control and treatment groups is depicted as \*  $P < 0.05$ , \*\*  $P < 0.01$ , and \*\*\*  $P < 0.001$ .



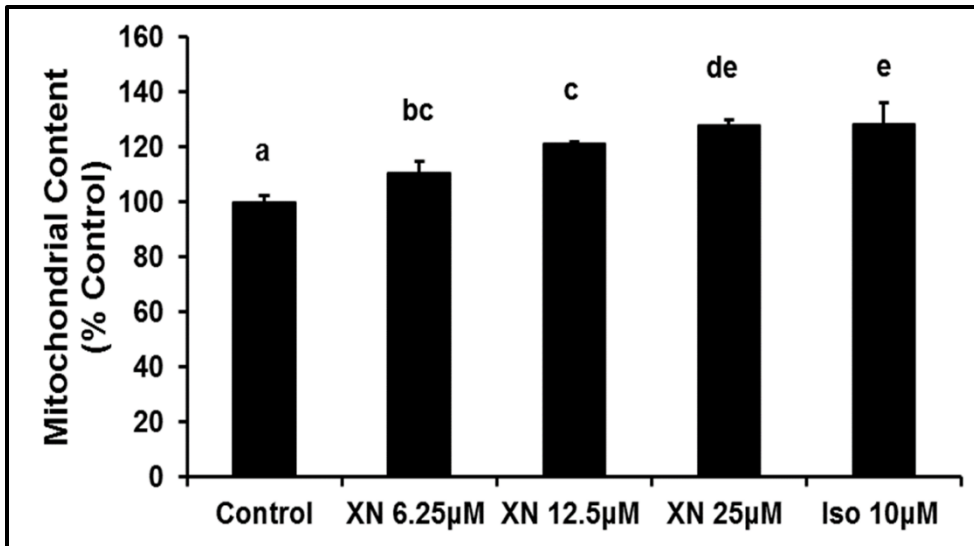


**Figure 8. XN increases mitochondrial content in 3T3-L1 mature adipocytes.** Various doses of xanthohumol (6.25, 12.5, and 25 µM) were administered to mature 3T3-L1 adipocytes, followed by quantification of mitochondrial content using MitoTracker™ Green FM assay. All data are presented as the mean ± SEM. Means denoted with different letters are statistically different,  $P < 0.05$ .

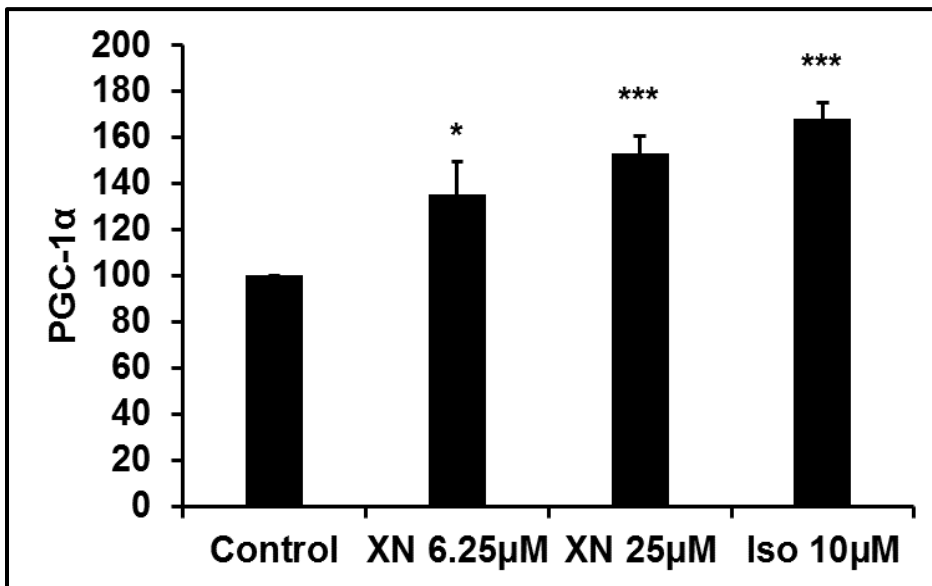
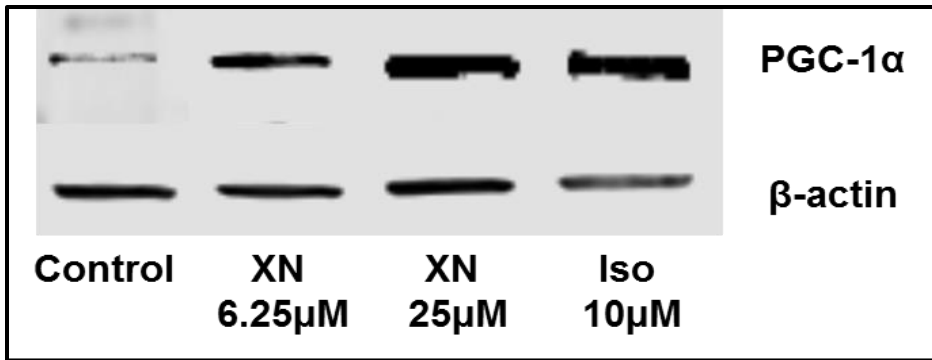


**Figure 9. XN increases the expression of PGC-1α, a regulator of mitochondrial metabolism.** Protein expression levels of PGC-1α in 3T3-L1 adipocytes after 24 hours of treatment with XN or isoproterenol. All data are presented as mean ± SEM. Statistical significance between control and treatment groups is depicted as \* P < 0.05, \*\*\* P < 0.001.

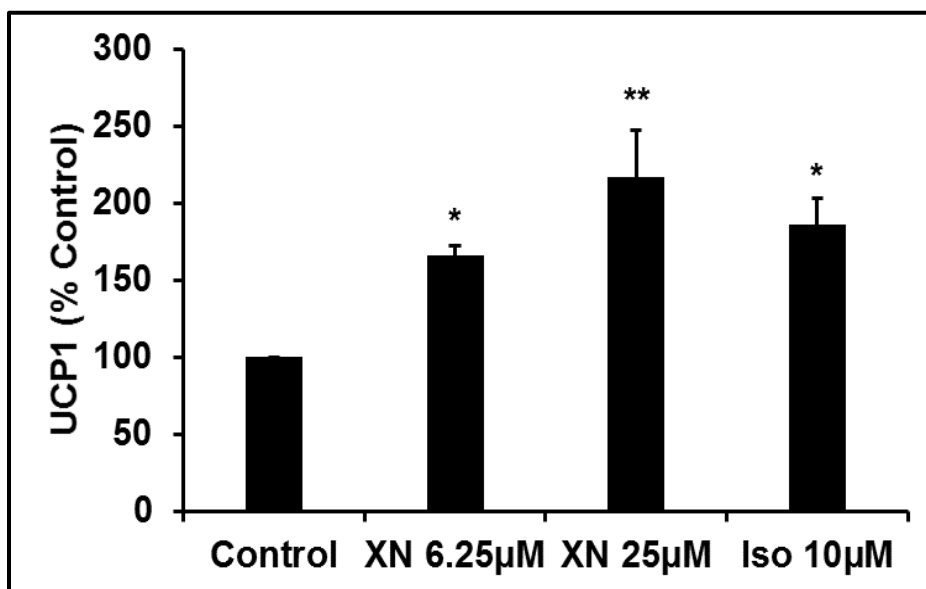
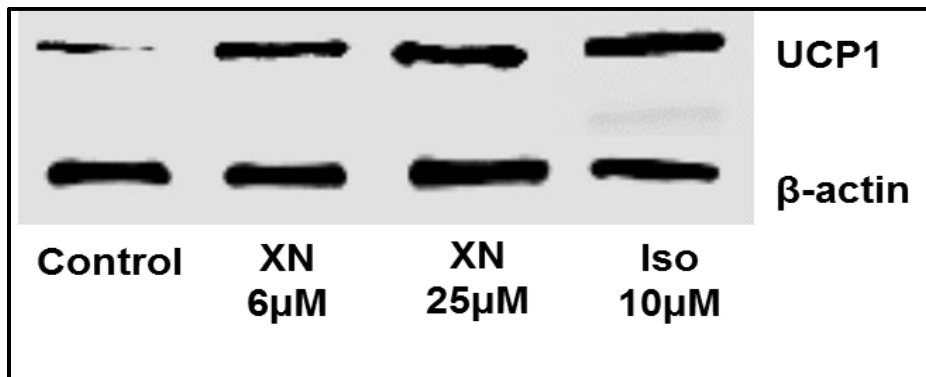


**Figure 10. XN treatment upregulates UCP1 expression.** Adipocytes were treated with XN or isoproterenol, and UCP1 expression levels were measured. All data are presented as mean  $\pm$  SEM. Statistical significance between control and treatment groups is shown as \*  $P < 0.05$ , and \*\*  $P < 0.01$ .

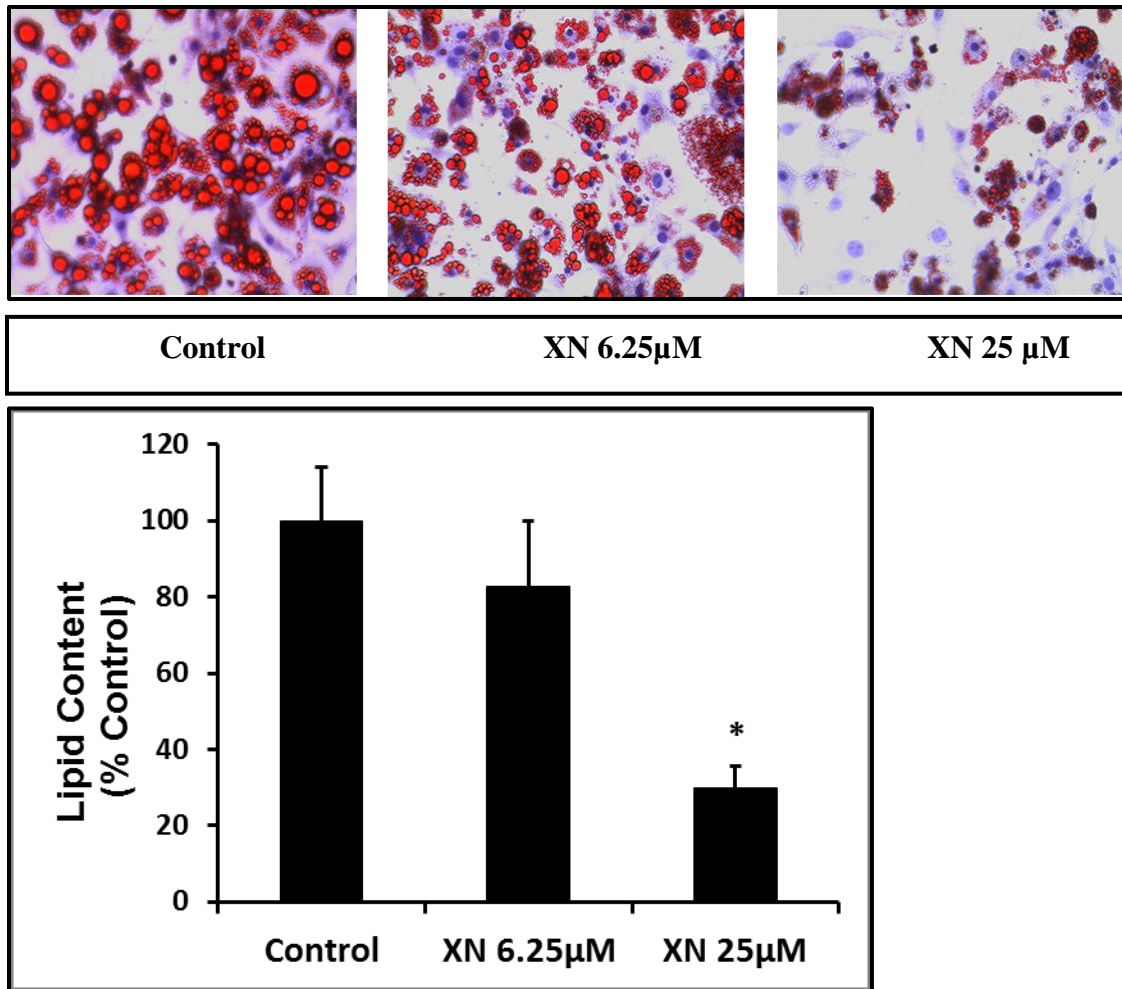


**Figure 11. XN inhibits preadipocyte differentiation and adipogenesis.** Oil Red O staining was performed to assess the maturation of 3T3-L1 adipocytes. XN treatment suppresses lipid accumulation in a dose-dependent manner. All data are presented as mean  $\pm$  SEM. Statistical significance between control and treatment groups is shown as \*  $P < 0.05$ .

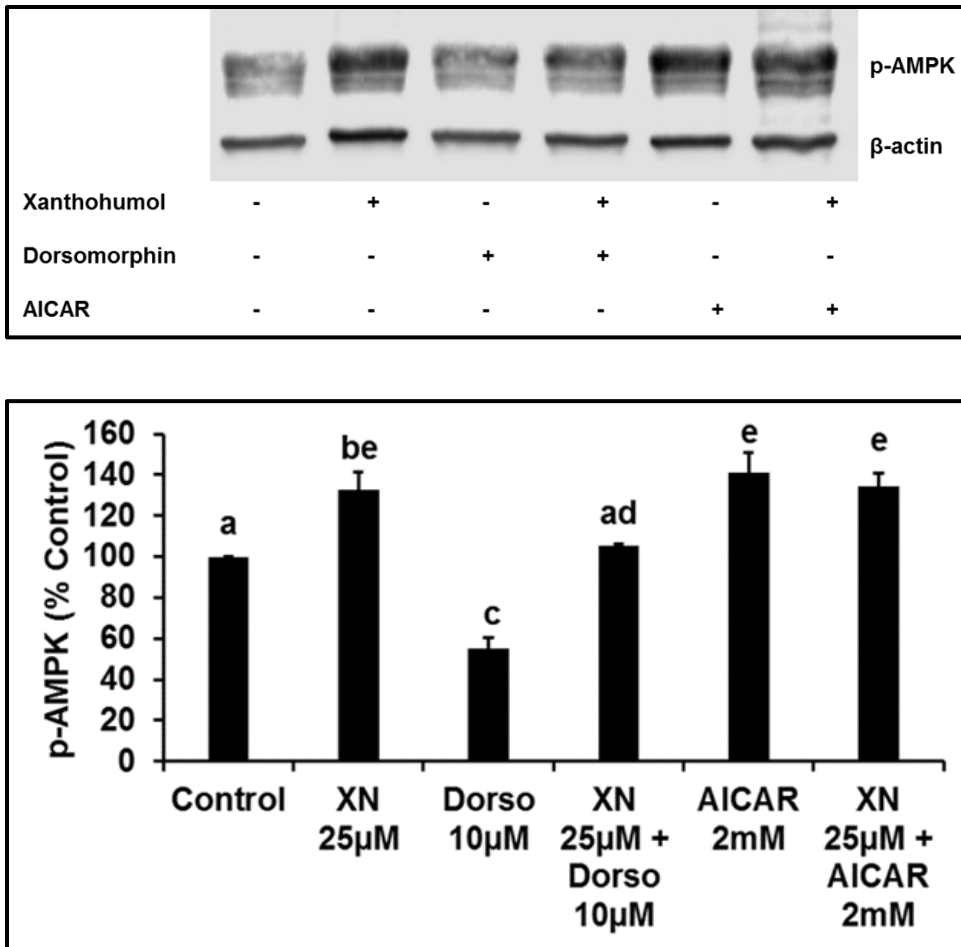


**Figure 12. Effect of XN, dorsomorphin, and AICAR on AMPK activation.** Mature adipocytes were treated for one hour and p-AMPK protein expression levels were measured. All data are presented as the mean  $\pm$  SEM. Means denoted with different letters are statistically different,  $P < 0.05$ .

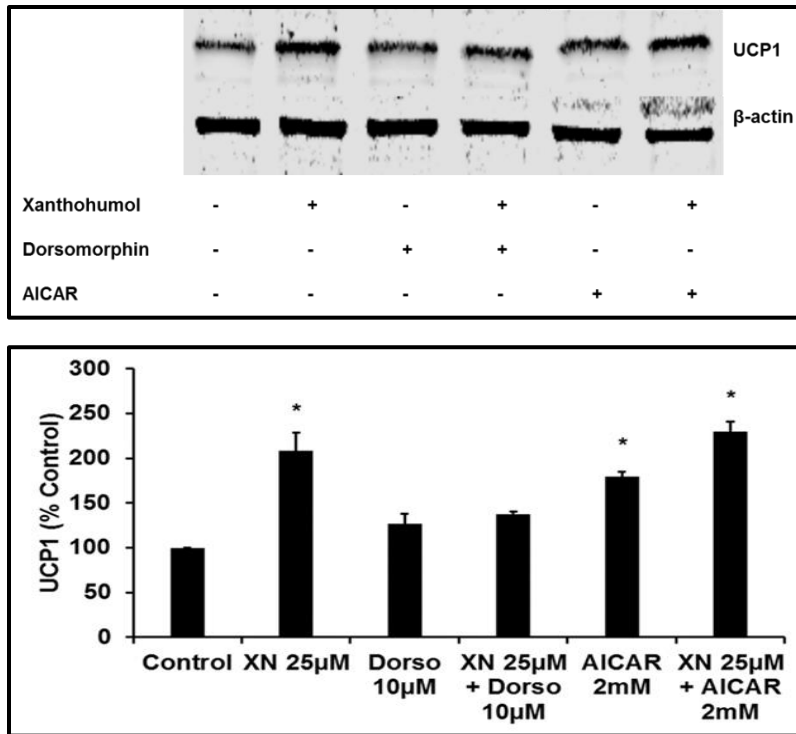


**Figure 13. XN-mediated upregulation of UCP1 is decreased in the presence of AMPK inhibitor, dorsomorphin.** AICAR (2 mM) and dorsomorphin (10  $\mu$ M) were incubated with mature adipocytes for one hour, and protein expression levels were determined by Western blotting. All data are presented as mean  $\pm$  SEM. Statistical significance between control and treatment groups is shown as \*  $P < 0.05$ .

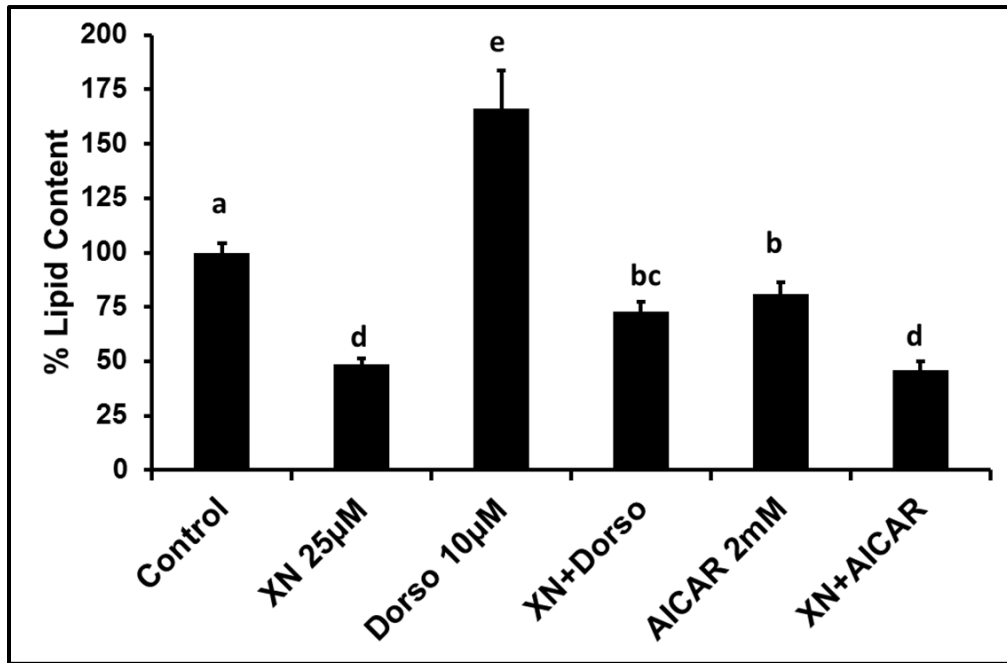


**Figure 14. XN-induced inhibition of adipogenesis is reversed in the presence of AMPK inhibitor, dorsomorphin.** 3T3-L1 preadipocytes were treated on day 0 until day 6 of maturation. Lipid accumulation was quantified by AdipoRed assay. All data are presented as the mean  $\pm$  SEM. Means denoted with different letters are statistically different,  $P < 0.05$ .

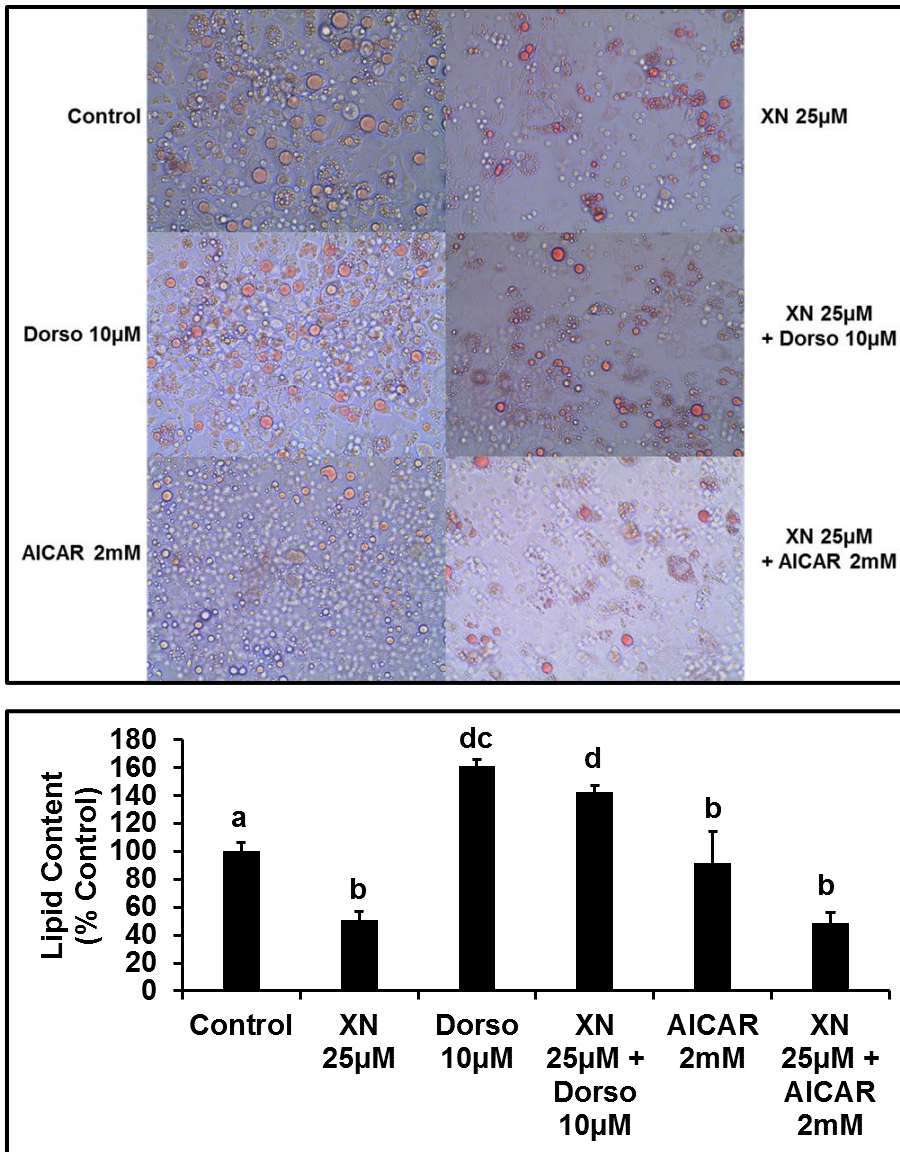


**Figure 15. Dorsomorphin reversed the XN-induced decrease in lipid content in mature 3T3-L1 adipocytes.** Mature 3T3-L1 adipocytes were treated on day 10 for 72 hours. Lipid accumulation was quantified by AdipoRed assay. All data are presented as the mean  $\pm$  SEM. Means denoted with different letters are statistically different,  $P < 0.05$ .



## **Chapter Three**

# **Xanthohumol Mediated Polarization of RAW264.7 Macrophages is Partly Mediated through the AMPK Signaling Pathway**

## Abstract

Anti-inflammatory, anti-oxidant, and anti-cancer effects of xanthohumol (XN), a prenylated chalcone extracted from common hop plants, are gaining attention and research has been expanding on the beneficial effects of this compound. In this study, we have investigated the anti-inflammatory effects of XN using a mouse monocytic cell line, RAW264.7. We hypothesized that the anti-inflammatory effects of XN are due to M2 polarization of macrophages which, in turn, is mediated partly through the adenosine monophosphate-activated protein kinase (AMPK) signaling pathway.

Our results suggest that XN upregulated the secretion of interleukin 10 (IL-10), a signature cytokine for M2 polarization, in RAW264.7 cells in a dose-dependent manner. We further demonstrated that XN increased arginase-1 expression, a marker for M2 polarization, and failed to increase inducible nitric oxide synthase (iNOS) expression, a marker for M1 polarization. XN decreased interferon- $\gamma$  (IFN- $\gamma$ ) induced elevation of nitrite release, indicating the inhibitory effects of XN against M1 polarization. Additionally, XN increased the secretion of catecholamines from macrophages comparable to interleukin 4 (IL-4), an inducer of the M2 phenotype. Finally, XN and AICAR upregulated the expression of p-AMPK and arginase-1 in RAW264.7 cells, indicating the role of AMPK signaling pathway in XN-induced effects.

Taken together, these results provide evidence for the anti-inflammatory properties of XN – mediated induction of M2 polarization. The M2 macrophage mediated anti-inflammatory effects, coupled with catecholamine secretion, and previously anti-adipogenic effects, makes XN an attractive molecule to study its beneficial effects on

metabolic diseases, like obesity and diabetes which are associated with underlying chronic, low-grade inflammation.

## 4.1 Introduction

Literature suggests that the imbalance of certain immune cells like macrophages and inflammatory adipokines, mediates the systemic inflammation that contributes to obesity [10, 74]. Macrophages respond to infection or the accumulation of dysfunctioning cells, which play a pivotal role in the regulation of inflammatory responses. Therefore, therapies that target macrophages may prevent or control inflammatory-mediated diseases, such as obesity.

Monocytes can undergo polarization towards either a pro-inflammatory macrophage or an anti-inflammatory macrophage in response to their microenvironment [75]. Classically activated M1 macrophages, stimulated by Th1 cytokines like IFN- $\gamma$  or the endotoxin lipopolysaccharide (LPS), produce effector molecules such as nitrogen intermediates and inflammatory cytokines. Alternatively activated M2 macrophages, stimulated by Th2 cytokines like IL-4, are characterized by their ability to produce catecholamines, arginase – 1, and IL-10 [76].

Flavonoids have been implicated in mediating inflammatory responses [77]. To date, research on XN's potential to regulate macrophage polarization is scarce. Our data shows that XN promotes monocytes to polarize towards the anti-inflammatory M2-like phenotype.

AMPK is a central controller of fatty acid, cholesterol, and glucose homeostasis through the phosphorylation of acetyl-CoA carboxylase, glycogen synthase, glucose transporter 4, HMG-CoA reductase, hormone sensitive lipase, and the mammalian target of rapamycin [64]. Adipose tissue macrophages (ATM) play a key role in obesity-induced inflammation. With increased pro-inflammatory cytokines in the obese state comes the activation of inflammatory pathways in metabolic tissues [78].

Macrophages are heterogenous in function and shift their properties and activation state based on their microenvironment. Activated AMPK has been shown to inhibit pro-inflammatory macrophage functioning and promote anti-inflammatory macrophage processes [43]. A potential role of AMPK in the suppression of inflammatory responses has been suggested using pharmacological approaches. To this end, we investigated the role of AMPK in the regulation of macrophage activity in response to XN stimulation. We demonstrate that AMPK is rapidly activated by XN in RAW264.7 cells and that AMPK mediates the macrophage inflammatory function.

## **4.2 Specific Aims**

Several flavonoids have been implicated in their ability to act as anti-inflammatory agents [79]. Macrophages have also been identified to release catecholamines as modulators of immune responses [80]. Macrophage polarization is a hot topic in the quest for new anti-obesity therapies.

As an energy sensor, AMPK is responsive to increased AMP/ATP ratios, pathogenic stressors, or energy imbalances. Recently, AMPK has been suggested to play a crucial role in regulating immune responses [65]. However, to date, XN and its

relationship with AMPK in modulating inflammatory responses has not been identified.

*In the current study, we will investigate whether XN regulates macrophage polarization and catecholamine secretion under the regulation of the AMPK pathway.*

*Specific Aim 1: To investigate the effects of XN on the polarization of RAW264.7 cells.*

*Specific Aim 2: To investigate the role of AMPK pathway in XN-induced polarization of RAW264.7 cells.*

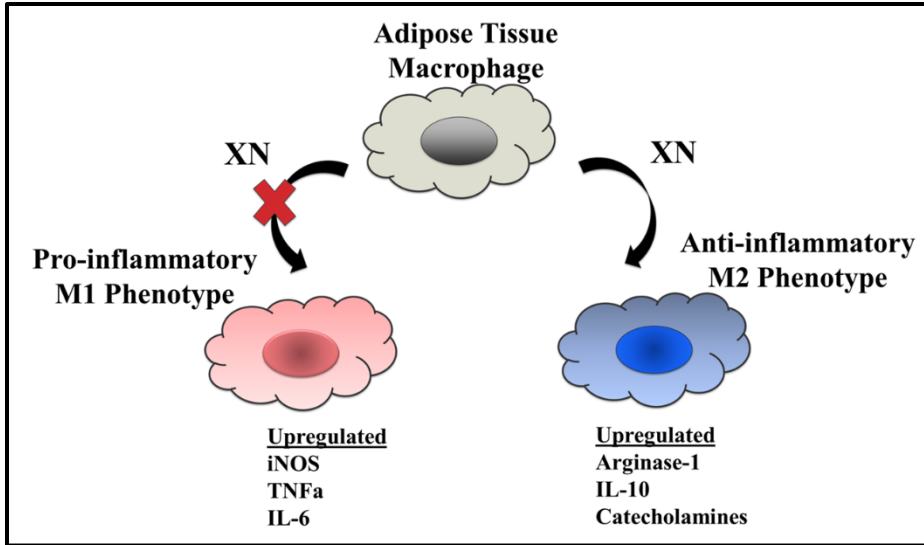


**Figure 16: Working model for XN-mediated polarization of macrophages.**

## **4.3 Materials and Methods**

### ***4.3.1 Cell culture***

The murine monocytic cell line, RAW264.7, was cultured in DMEM containing 10% FBS and 1% PS at 37°C in a 5% CO<sub>2</sub> incubator. Medium was replaced every other day. Cells were passaged at passage numbers 4 or 5 every four days in 0.25% trypsin plus EDTA. RAW264.7 cells were seeded at a density of 1.0 x 10<sup>6</sup>/mL in 6-well plates. Once the cells reached 100% confluency, they were treated with 0.1% DMSO, XN 6.25 μM or 25 μM, IFN-γ 10ng/mL, or IL-4 20ng/mL for 24 hours. To investigate AMPK's role in XN-mediated polarization, RAW264.7 cells were treated with 0.1% DMSO, XN 6.25 μM or 25 μM, AICAR 2 mM, dorsomorphin 10 μM, or IL-4 20ng/mL for one hour.

### ***4.3.2 Cytotoxicity***

Confluent RAW264.7 cells were treated with 0.1% DMSO vehicle control or XN for 24 hours. Cell viability was measured using Prestoblu<sup>TM</sup> Cell Viability Reagent according to the manufacturer's protocol. The absorbance of metabolically active cells was quantified 1 hour after incubation in the reagent using the Biotek Synergy HT microplate reader at 570nm.

### ***4.3.3 Immunoblot analysis***

Proteins were lysed and extracted from RAW264.7 macrophages after treatment with 0.1% DMSO, XN 6.25-25 μM, IFN-γ 10ng/mL, or IL-4 20ng/mL for 24 hours or AICAR 2 mM or dorsomorphin 10 μM for one hour. Details are provided in chapter two (page 25). Primary antibodies included: anti-iNOS, anti-β-actin (Santa Cruz



Biotechnology, Cambridge, MA, USA), anti-arginase – 1, and p-AMPK (Thr172) (all from Abcam, Cambridge, MA, USA).

#### ***4.3.4 Enzyme-linked Immunosorbent Assays***

Catecholamine levels in culture medium of XN and IL-4 treated samples were determined by ELISA, following the manufacturer's protocol (Blue Gene for Life Science; Shanghai, China). Monoclonal mouse anti-catecholamine antibodies were used as capturing antibodies.

The product of the enzyme-substrate reaction produces a color change and these color changes were determined via the Synergy Biotek HT microplate reader at 450nm. Standard curves were utilized to analyze the color intensity with the concentration of catecholamine secretion from the standards.

For IL-10 levels, culture supernatants of XN and IL-4 treated RAW264.7 macrophages were processed following the manufacturer's instructions using a mouse IL-10 ELISA kit (R&D Systems; Minneapolis, MN, USA).

#### ***4.3.5 Nitrite Release Assay***

XN, IFN- $\gamma$  with or without XN, and IL-4 RAW264.7 culture supernatants were analyzed for nitrite release based on the Greiss reaction (Promega; Madison, WI, USA). Nitrite accumulation is an indicator of nitric oxide synthesis, and this accumulation is responsible for the cytotoxic mediators released from macrophages [81].

Culture supernatant (50uL) was incubated at room temperature with Greiss reagent in a 96-well plate. After 10 minutes, absorbance was read on the Synergy Biotek

HT microplate reader at a wavelength of 520nm. Nitrite concentrations were calculated in comparison to a standard curve.

#### ***4.3.6 Statistical analysis***

All data were expressed as the mean  $\pm$  SEM. All assays were performed in triplicate for a minimum of three independent experiments. Comparisons were made by using one-way ANOVA on GraphPad Prism software, followed by Tukey's post hoc tests. Statistical significance was reported as \*  $P < 0.05$ , \*\*  $P < 0.01$ , \*\*\*  $P < 0.001$  or \*\*\*\*  $P < 0.0001$ .

### **4.4 Results**

#### ***4.4.1 High dose XN decreases cell viability in RAW264.7 cells***

The biological functions of a cell can largely depend on its viability. The effect of XN on the viability of RAW264.7 cells is depicted in Fig. 17. At low dose ranges (6.25, 12.5, and 25  $\mu$ M), XN had no significant effect on cell viability after 24 hours of treatment. However, at higher doses (50 and 75  $\mu$ M), XN significantly decreased cellular viability of RAW264.7 cells by  $37\% \pm 0.65$  and  $43\% \pm 0.65$ , respectively. Thus, XN 6.25 and 25  $\mu$ M was employed in our experiments.

#### ***4.4.2 XN treatment leads to M2 macrophage polarization in RAW264.7 cells***

It has been recently recognized that XN has anti-inflammatory properties [82]. To study XN's possible anti-inflammatory effects in macrophage polarization, RAW264.7 cells were stimulated with XN or IL-4 for 24 hours.

Arginase – 1, an anti-inflammatory M2 macrophage marker, protein expression levels were measured via Western blotting. Our results show that XN significantly upregulates the expression of arginase – 1, in a dose-dependent manner ( $P < 0.0001$ ). Furthermore, XN 25  $\mu$ M exhibited pronounced arginase – 1 upregulation comparable to that of IL-4, a positive control for M2 macrophage polarization (Fig. 18). These results suggest that XN polarizes RAW264.7 cells towards the anti-inflammatory phenotype.

#### ***4.4.3 XN induces catecholamine and IL-10 secretion from RAW264.7 cells***

To investigate whether XN stimulates IL-10 and free catecholamine secretion from macrophages, RAW264.7 cells were treated with 0.1% DMSO control, XN 6.25-25  $\mu$ M, or IL-4 for 24 hours. XN significantly increases the release of catecholamines (Fig. 19) and IL-10 (Fig. 20) levels in a dose-dependent manner, providing novel evidence for XN-induced M2 polarization.

#### ***4.4.4 XN inhibits M1 polarization in RAW264.7 cells***

The effects of XN on iNOS expression in macrophages stimulated with IFN- $\gamma$  were investigated in RAW264.7 cells treated with XN in the presence or absence of IFN- $\gamma$ . As shown in Fig. 21A, iNOS protein expression was increased in IFN- $\gamma$  stimulated RAW264.7 cells. XN at 25  $\mu$ M decreased IFN- $\gamma$ -induced upregulation of iNOS thus, inhibiting M1 polarization. IFN- $\gamma$  activated macrophages significantly induced the release of nitrite but this effect was suppressed by XN (Fig. 21B).

#### ***4.4.5 XN activates AMPK in RAW264.7 cells***

We performed Western blot analyses to evaluate the effect of XN on AMPK phosphorylation in XN, IL-4, AICAR, and dorsomorphin treated RAW264.7 cells. We first examined whether XN led to AMPK activation after one hour of treatment. Fig. 22 shows that XN significantly upregulated the expression of p-AMPK. Additionally, AICAR increased the expression of p-AMPK. In contrast, dorsomorphin attenuated the activation of p-AMPK in RAW264.7 cells.

#### ***4.4.6 XN-induced M2 polarization is dependent upon the activation of AMPK signaling pathway***

We next evaluated the impact of enhanced AMPK activation on macrophage inflammatory activity. RAW264.7 cells were treated with XN, AICAR, or IL-4 and analyzed for arginase – 1 protein expression. AICAR treated RAW264.7 cells displayed significant amounts of arginase – 1 expression comparable to that of both IL-4 and XN (Fig. 23). This data suggests that AMPK regulates XN-induced macrophage polarization.

### **4.5 Discussion**

Obesity, a central modulator of the metabolic syndrome, is closely linked with the state of chronic, low-grade inflammation. In adipose tissue, excessive energy intake results in pro-inflammatory macrophages infiltration and a shift in the phenotype polarization of macrophages. Literature has demonstrated that disruption in the expression of pro-inflammatory cytokines released by M1 macrophages relieves adipose

tissue inflammation and dysregulation [83]. To this end, it was our goal to examine the effects of XN on macrophage polarization.

Macrophages are well characterized key regulators of the inflammatory response [84, 85]. Numerous studies have reported that macrophage infiltration in adipose tissue initiates and accelerates the cycle of inflammation within the obese state [42, 86]. Gordon et al., reported that both pro-inflammatory and anti-inflammatory macrophages reside in the tissue of obese persons [87]. Moreover, it has been accepted that the manipulation of the M1/M2 ratio, such that M1 macrophages are decreased in numbers and M2 macrophages are increased, ameliorates adipose tissue inflammation [88]. In the current study, we demonstrate that XN ameliorates inflammation and regulates macrophage polarization through the AMPK signaling pathway.

XN, a hops flavonoid, has been studied extensively for its anti-carcinogenic, anti-oxidant, and anti-diabetic properties [4]. XN has also been reported to inhibit iNOS expression resulting in suppressed nitric oxide production in macrophages [89]. Adipose tissue marked with inflammation, orchestrated by ATM recruitment, is the central event initiating the metabolic syndrome [78]. To this end, we investigated whether XN polarizes RAW264.7 cells and the molecular mechanism behind it.

Recent studies have implicated flavonoids as having potent anti-inflammatory properties. The dietary flavonoid quercetin was shown to prevent M1 polarization and inflammation of ATMs [90]. Resveratrol exerts anti-inflammatory effects on adipose tissue by attenuating tumor necrosis factor- $\alpha$  in visceral white adipose tissue macrophage release in mice [91]. Gao et al., reported that curcumin induces M2 polarization by IL-4

or IL-13 secretion in RAW264.7 cells [92]. In accordance with these findings, our data show that XN promotes RAW264.7 cells towards the anti-inflammatory phenotype as demonstrated by increased arginase – 1 expression, catecholamine, and IL-10 secretion. Conflictingly, isoliquiritigenin, a flavonoid from licorice, has been demonstrated to inhibit M2 polarization [93].

To further identify XN's anti-inflammatory characteristics, we showed that XN attenuates pro-inflammatory mediators in RAW264.7 cells. IFN- $\gamma$ -induced iNOS protein expression was reversed by XN. Furthermore, XN suppressed the release of nitrite in IFN- $\gamma$  stimulated RAW264.7 macrophages. These results are suggestive of XN's capability to prevent the polarization of macrophages towards the pro-inflammatory M1-like phenotype. In conclusion, XN could improve obesity associated inflammation via regulation of the M1/M2 ratio in adipose tissue. Therefore, identifying signaling pathways that regulate macrophage polarization can help lead to strategies for the modification of macrophage behavior.

The aim of this study was focused on addressing the hypothesis that the energy sensor, AMPK, serves as a regulator of inflammation in macrophages. Inflammation is the orchestrator in obesity pathogenesis and macrophage inflammation is the key component of obesity-induced inflammation. We believe that the signaling protein, AMPK, modulates immunometabolism because it is abundantly expressed in both adipocytes and macrophages, regulated by inflammatory stimuli, and regulates free fatty acid metabolism and the inflammatory response.

AMPK inhibits anabolic processes and activates catabolic processes once activated. A proposed role for AMPK in the regulation of inflammatory responses is supported by the use of AICAR; AICAR was shown to suppress the synthesis of iNOS by macrophages and adipocytes [94]. Several activators of AMPK have been identified to decrease pro-inflammatory mediators such as IFN- $\gamma$  and tumor necrosis factor- $\alpha$  [94-96]. Furthermore, Sag et al., reported that AMPK promotes macrophages towards the anti-inflammatory M2 phenotype [43]. This supports our results that XN and AICAR upregulated p-AMPK and arginase – 1 levels in RAW264.7 cells. These results indicate that XN-mediated macrophage polarization is dependent upon the activation of the AMPK signaling pathway.

Our data indicate that AMPK is a regulator of immunometabolism in RAW264.7 cells stimulated with XN. Disturbances of AMPK signaling during adipose tissue dysfunction could be linked to the over-productive activation of inflammatory signaling in obesity.

#### 4.6 Figures

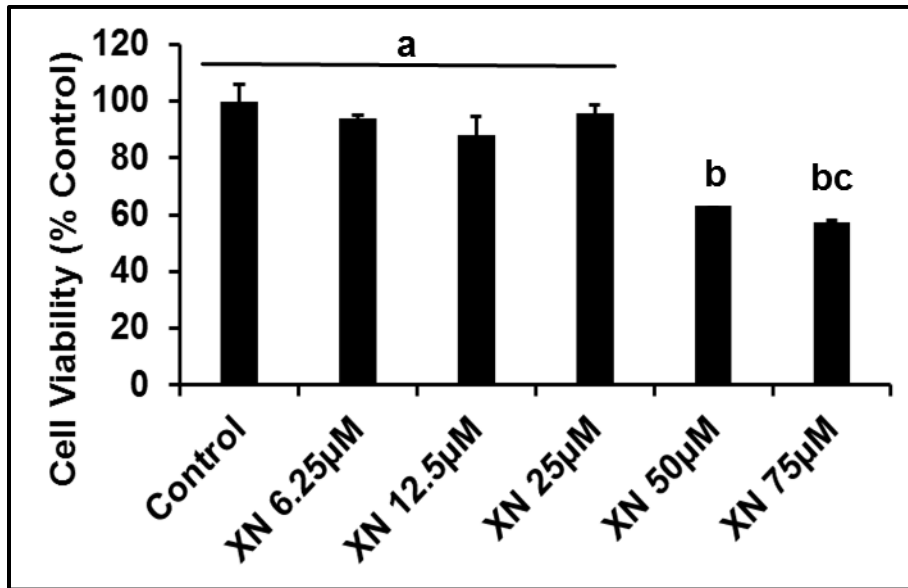


**Figure 17. Effect of XN on RAW264.7 cellular viability.** RAW264.7 cells were treated with varying concentrations of XN for 24 hours and cell viability was measured by Prestoblue™ Cell Viability Reagent. All data are presented as the mean  $\pm$  SEM. Means denoted with different letters are statistically different,  $P < 0.05$ .



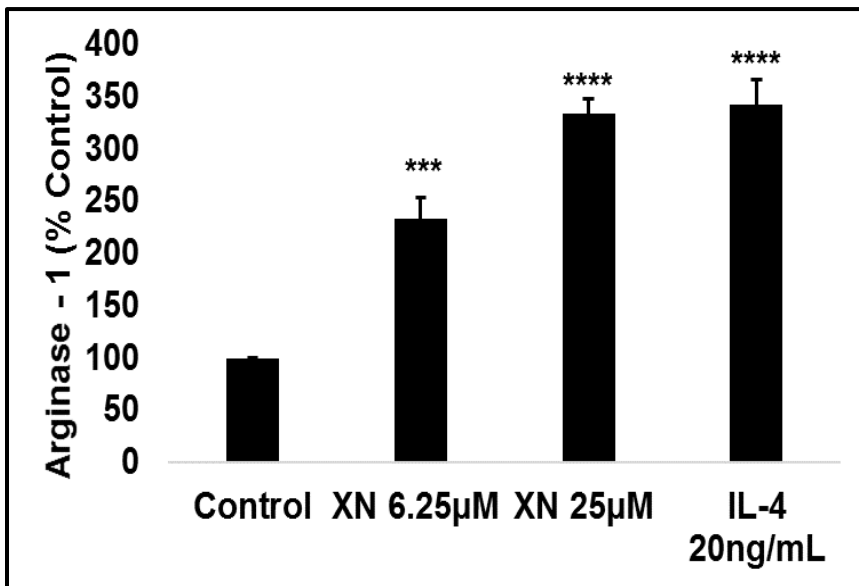
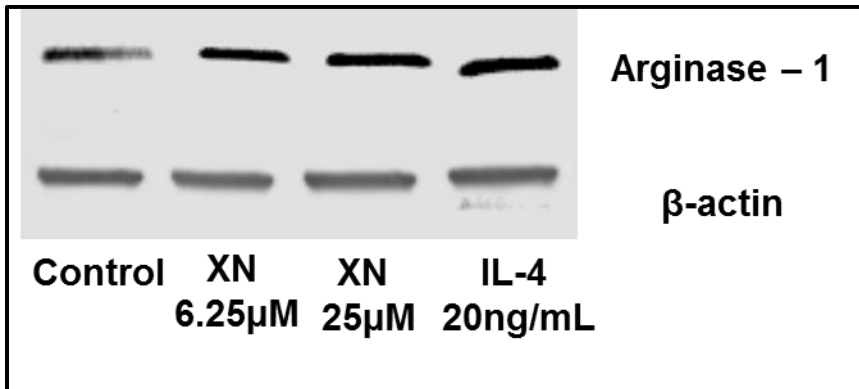


**Figure 18. Effect of XN on arginase – 1 protein expression levels.** RAW264.7 cells were treated with varying concentrations of XN and IL-4 as a positive control and arginase – 1 expression was determined by Western blot. All data are presented as mean  $\pm$  SEM. Statistical significance between control and treatment groups is represented as \*\*\* P < 0.001, \*\*\*\* P < 0.0001.

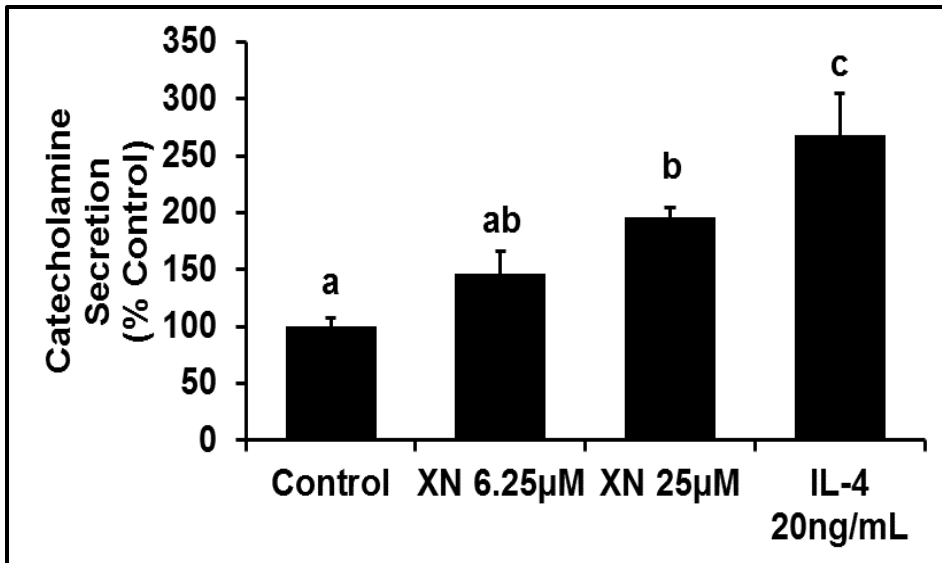


**Figure 19. XN induces catecholamine secretion in RAW264.7 cells.** RAW264.7 cells were treated with vehicle, XN, or IL-4 for 24 hours and catecholamine synthesis was examined. All data are presented as the mean  $\pm$  SEM. Means denoted with different letters are statistically different,  $P < 0.05$ .

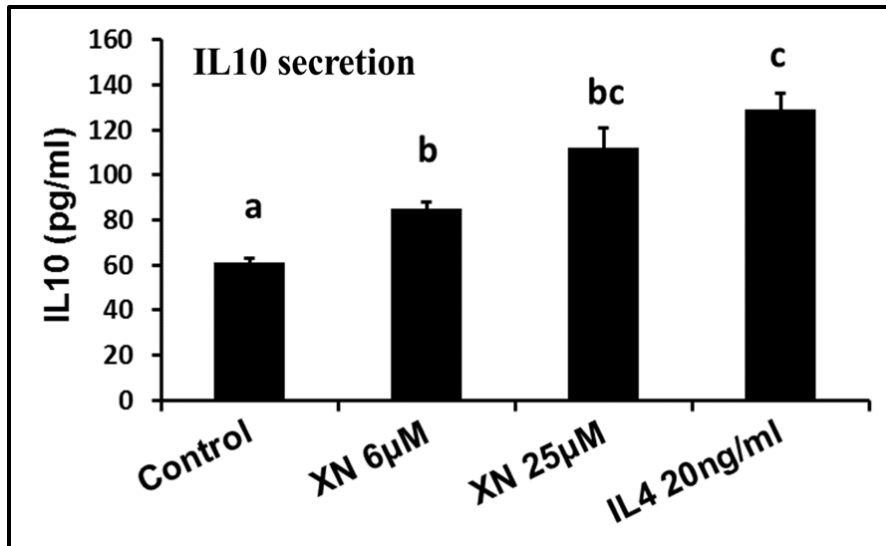


**Figure 20.** Effect of XN on IL-10 secretion in RAW264.7 cells. All data are presented as mean  $\pm$  SEM. Means denoted with different letters are statistically different,  $P < 0.05$ .

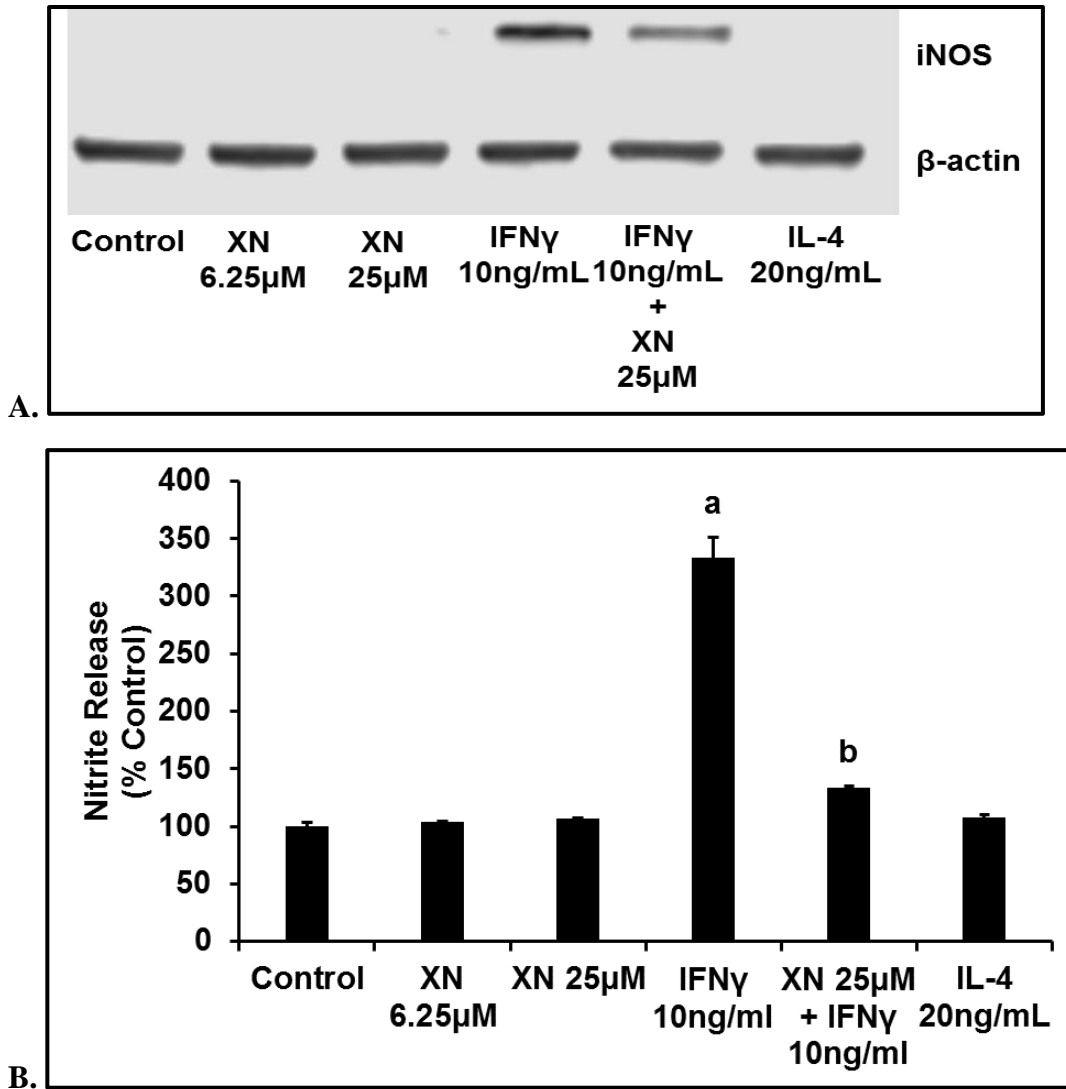


**Figure 21. XN prevents M1 polarization in RAW264.7 cells.** RAW264.7 cells were treated with XN, IL-4, or IFN- $\gamma$  in the presence or absence of XN for 24 hours. **A.** XN downregulated IFN- $\gamma$ -induced iNOS expression. **B.** XN suppressed nitrite release in IFN- $\gamma$  activated RAW264.7 macrophages. All data are presented as mean  $\pm$  SEM. Means denoted with different letters are statistically different,  $P < 0.05$ .

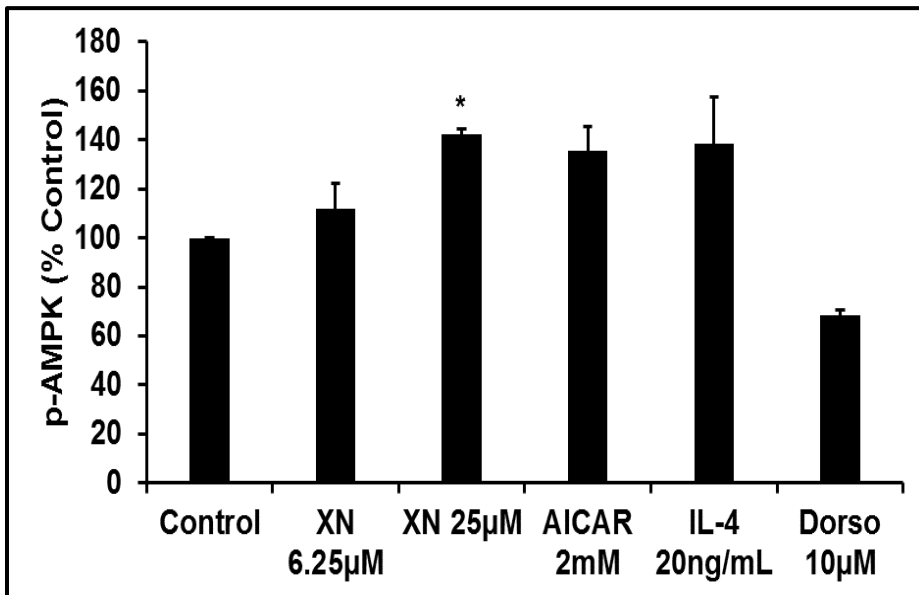
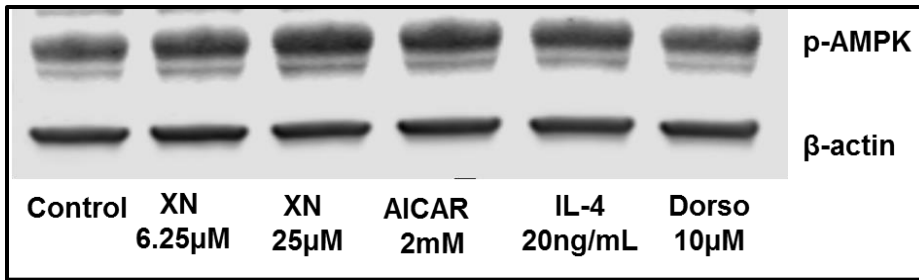


**Figure 22. Effect of XN on p-AMPK protein expression.** RAW264.7 cells were treated with XN, AICAR, IL-4, or dorsomorphin for one hour and p-AMPK expression levels were assessed by Western blotting. All data are presented as mean  $\pm$  SEM. Statistical significance between control and treatment groups is represented as \*  $P < 0.05$ .

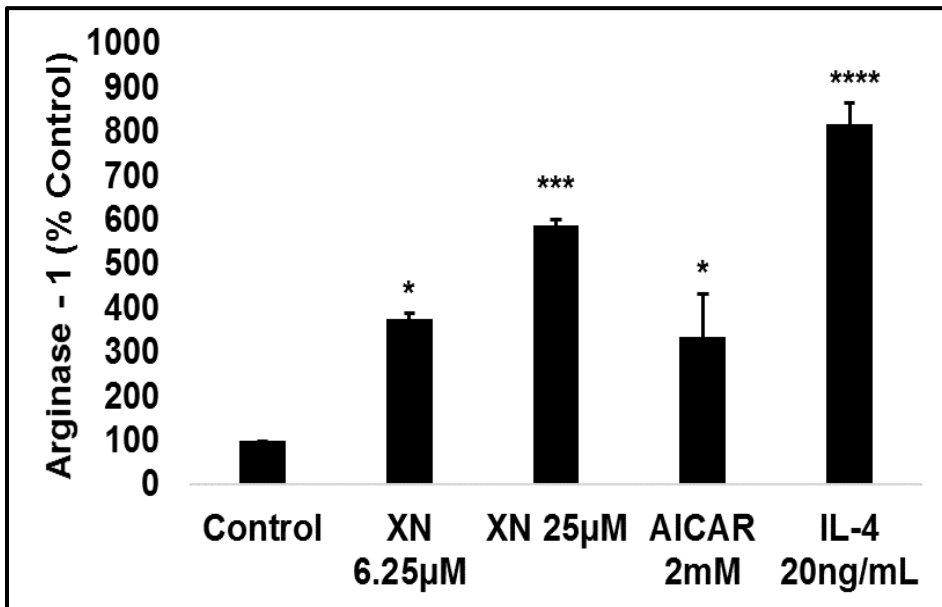
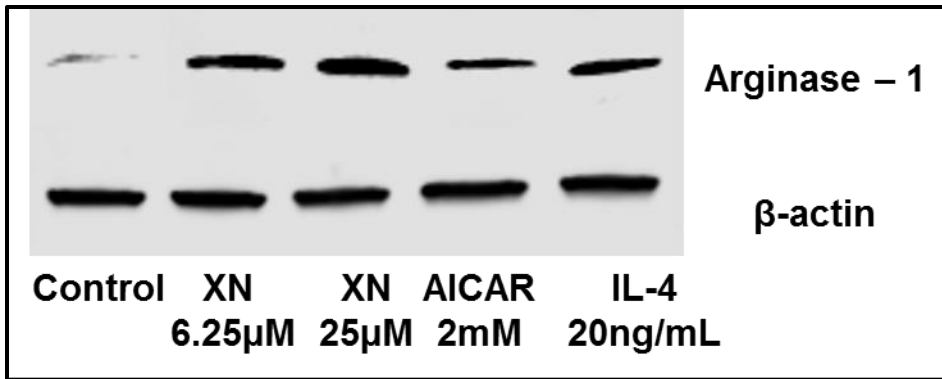


**Figure 23. Effect of XN and AICAR on arginase-1 expression.** RAW264.7 cells were treated with AICAR or XN for one hour and arginase-1 protein expression levels were measured via Western blotting. All data are presented as mean  $\pm$  SEM. Statistical significance between control and treatment groups is represented as \*  $P < 0.05$ , \*\*\*  $P < 0.001$ , \*\*\*\*  $P < 0.0001$ .

## **Chapter Four**

### **Direct and Indirect Effects of Xanthohumol on the Induction of Beiging in 3T3-L1 adipocytes**

## 6.1 Introduction

A marked feature of obesity is hypertrophic and hyperplastic adipocytes, and adipose tissue that is mainly comprised of pro-inflammatory M1 macrophages. Adipokines and cytokines derived from adipocytes and macrophages, respectively, cross-talk may result in the metabolic syndrome. It has been proposed that the paracrine loop, with the key players being free fatty acids and pro-inflammatory cytokines, aggravates inflammation and promotes the hypertrophy of adipocytes [83].

Noteworthy, similar changes in inflammation are remarkable in fat depots [97]. Adipocytes analyzed for gene expression profiles obtained from obese mice and humans showed that macrophages contribute the majority of pro-inflammatory cytokines [42]. These observations lead to the conclusion that adipose tissue macrophages are the sole source of inflammation in obesity.

Mammals sustain energy homeostasis via thermogenesis, activated by cold exposure. When the central nervous system detects cold temperatures, the sympathetic nervous system will become activated and release catecholamines in BAT and WAT [98]. This release of catecholamines stimulates thermogenesis in brown/beige adipocytes. Nguyen et al., demonstrated that M2 macrophages regulate thermogenesis and in turn, the beiging of white adipocytes [76].



With this, we aim to investigate the cross-talk between adipocytes and macrophages within a transwell co-culture system to measure beiging stimulated by XN, and determine inflammatory changes. Our data suggests that XN and IL-4 induced UPC1 expression and increased mitochondrial biogenesis in adipocytes co-cultured with macrophages, suggesting that RAW264.7 cells mediated XN-induced beiging of adipocytes. Furthermore, XN stimulated the secretion of catecholamines and IL-10 in the co-culture system, confirming the acquisition of the M2 macrophage phenotype.

## **6.2 Specific Aims**

Adipose tissue is characterized by excessive inflammation in the obese state. The paracrine loop between adipocytes and macrophages exacerbates this inflammation in obese adipose tissue. Phytochemicals have been identified to have anti-adipogenic and anti-inflammatory effects but little is known about the effect of XN within a co-culture system.

*Specific Aim 1: To establish a co-culture system comprised of 3T3-L1 adipocytes and RAW264.7 macrophages.*

*Specific Aim 2: To demonstrate direct and indirect effects of XN leading to enhanced induction of beiging in 3T3-L1 adipocytes.*

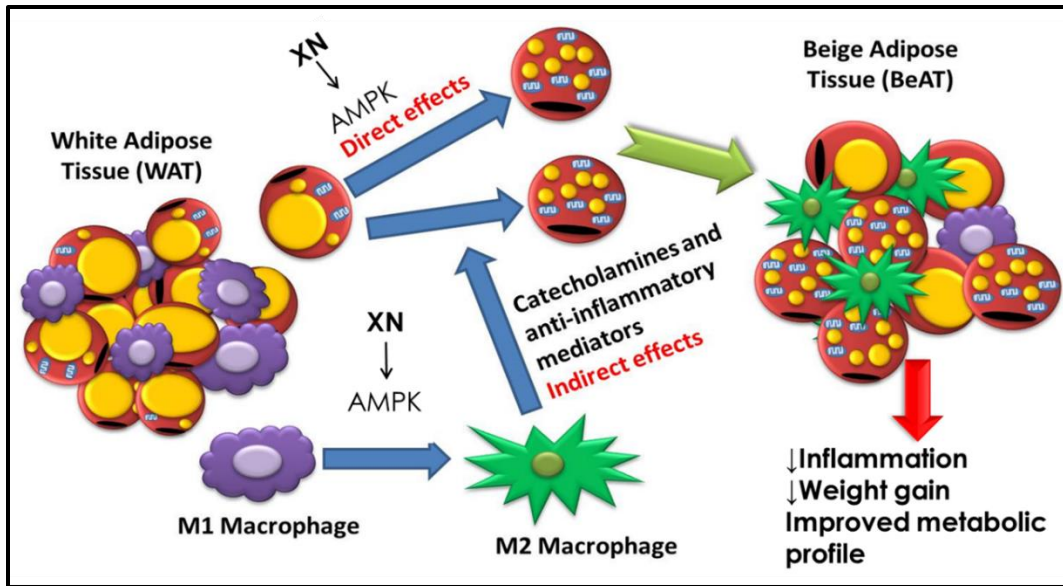


Figure 24. Working model demonstrating the direct and indirect effects of XN on the induction of beigeing in WAT.

## **4.3 Materials and Methods**

### ***4.3.1 Cell Culture and Differentiation of 3T3-L1 adipocytes and RAW264.7 cells***

Detailed cell culturing for 3T3-L1 adipocytes and RAW264.7 cells are described in chapter two (page 30) and chapter three (page 6), respectively.

### ***4.3.2 Transwell Co-culture System***

3T3-L1 preadipocytes were grown to confluency in 6-well plates and differentiated to mature adipocytes as described above. Cells were then cultured in a transwell system, on day 5 of the adipocyte maturation cycle, with 3T3-L1 cells in the lower chamber and RAW264.7 cells seeded onto the 0.4 $\mu$ m cell insert (Corning Incorporated; Kennebunk, ME, USA). The insert of the transwell is porous in that these pores are small enough to prevent the passage of most cell types, yet large enough to permit the passage of small molecules like cytokines or adipokines. Within the co-culture system, RAW264.7 cells were directly treated with 0.1% DMSO vehicle control, XN, or IL-4 for 24 hours.

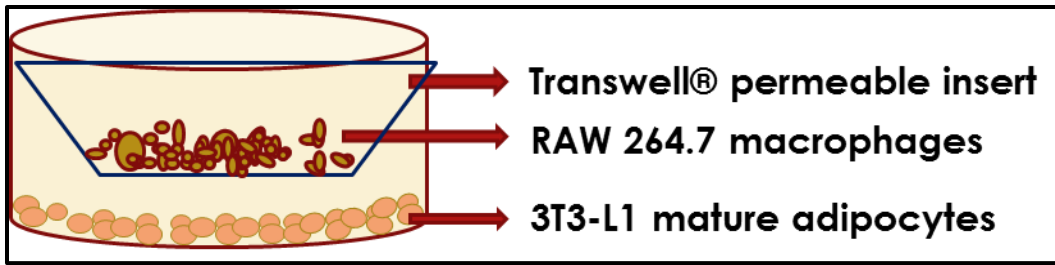


**Figure 25. Illustration of transwell co-culture system.**

#### ***6.3.4 Immunoblot Analysis***

Immunoblot analysis was carried out as described in chapter 2 (page 25).

#### ***6.3.5 Mitochondrial biogenesis***

Mature 3T3-L1 adipocytes co-cultured with RAW264.7 cells were treated with 0.1% DMSO, XN25  $\mu$ M, or IL-4 20 ng/mL for 24 hours and incubated with Mitotracker® Green FM (Invitrogen, Grand Island, NY, USA) as per the manufacturer's instructions. Mitochondrial activity was measured using the Biotek Synergy HT (Winooski, VT, USA) microplate reader at 516nm and images were captured using the EVOS FL Auto Imaging System (ThermoFisher Scientific, Grand Island, NY, USA) microscope.

#### ***6.3.6 Enzyme-linked Immunosorbent Assays***

Detailed methods are described in chapter three (page 51).

#### ***6.3.7 Statistical analysis***

All data were expressed as the mean  $\pm$  SEM. All assays were performed in triplicate for a minimum of three independent experiments. Comparisons were made by using One-way ANOVA on GraphPad Prism software, followed by Tukey's post hoc tests. Statistical significance was reported as \*  $P < 0.05$ , \*\*  $P < 0.01$ , \*\*\* $P < 0.001$  or \*\*\*\*  $P < 0.0001$ .

## **6.4 Results**

### ***6.4.1 Enhanced levels of UCP1 in 3T3-L1 adipocyte-macrophage co-culture upon XN stimulation***

We investigated the expression of UCP1 within mono-cultured adipocytes and co-cultured RAW264.7 cells and white adipocytes. We observed less pronounced levels of UCP1 protein expression in XN treated 3T3-L1 adipocytes cultured alone (Fig. 26A) than in XN-stimulated 3T3-L1 mature adipocytes co-cultured with RAW264.7 cells (Fig. 26B). Therefore, macrophages had an indirect impact on the beiging of differentiated adipocytes.

### ***6.4.2 XN increased mitochondrial biogenesis in 3T3-L1 adipocytes co-cultured with RAW264.7 macrophages***

Because mitochondrial biogenesis is a feature of brown/beige adipocytes, we sought to investigate mitochondrial biogenesis activity within this co-culture system.

Our data show that XN induced the upregulation of mitochondrial biogenesis in 3T3-L1 adipocytes co-cultured with RAW264.7 macrophages,  $P < 0.05$  (Fig. 27). This confirms beiging in this co-cultured transwell model.

### ***6.4.3 XN induces catecholamine secretion in co-cultured cells***

Next, to investigate whether this beiging of 3T3-L1 adipocytes co-cultured with RAW264.7 cells was a result of macrophage polarization, we first examined the effect of XN on catecholamine secretion. The release of catecholamines into the co-culture medium increased with 24 hours of XN treatment (Fig. 28). Interestingly enough, these

effects were not more pronounced than catecholamine secretion in RAW264.7 macrophages cultured alone (Fig. 19).

#### ***6.4.4 Indirect contact between macrophages and adipocytes enhances secretion of anti-inflammatory IL-10 levels***

To determine if anti-inflammatory IL-10 secretion is regulated by paracrine communications, we co-cultured RAW264.7 macrophages, treated with XN or IL-4, with 3T3-L1 adipocytes. Significant differences in IL-10 secretion levels were found when comparing direct (Fig. 20) and indirect macrophage-adipocyte co-cultures (Fig. 29), indicating that the co-culturing of cells in transwells, increased XN-induced IL-10 levels by 551%.

Noteworthy, when comparing IL-4-stimulated RAW264.7 mono-cultured IL-10 levels to co-cultured IL-10 levels, IL-10 secretion levels were more pronounced by 1,644%, suggesting that adipocytes may secrete IL-10 [99] and XN is mediating inflammatory responses in both cell lines.

### **6.5 Discussion**

Obesity is associated with chronic, low-grade inflammation. Studies have demonstrated that dysfunctional adipose tissue is infiltrated with pro-inflammatory macrophages [42]. In the current study, we developed an *in vitro* transwell co-culture system comprised of differentiated 3T3-L1 adipocytes and RAW264.7 macrophages stimulated with XN or IL-4.

In the lean state, adipose tissue is comprised mostly of M2-like macrophages while in the obese state, M1-like macrophages infiltrate adipose tissue. This infiltration creates the state of chronic, low-grade inflammation marked by obesity and this polarization state is characterized by secretions of pro-inflammatory cytokines [100]. Relative reductions in type 2 immunity may generate increases in pro-inflammatory macrophage polarization in obesity, influencing adipose tissue dysfunction and hormone response.

Studies have proposed that M2 macrophages and type 2 immune signaling pathways leads to the beiging of white fat [76, 101]. It has been demonstrated that IL-4 induces the expression of tyrosine hydroxylase, the rate-limiting enzyme in the synthesis of catecholamines, in M2 macrophages, increasing beiging of white adipose tissue [101]. In the present study, we observed a lack of significant IL-4-stimulated catecholamine secretion within the adipocyte-macrophage co-culture system, whereas unpublished data from Dr. Rayalam's lab suggests that conditioned media experiments with RAW264.7 cell culture supernatant and mature 3T3-L1 adipocytes increased catecholamine secretion levels. This study demonstrates, for the first time, XN-induced polarization of macrophages toward the anti-inflammatory phenotype beiges WAT as demonstrated by enhanced IL-10 secretion, UCP1 expression, and mitochondrial biogenesis within the transwell co-culture system, mediating XN's multi-faceted anti-obesity effects.



## 6.6 Figures

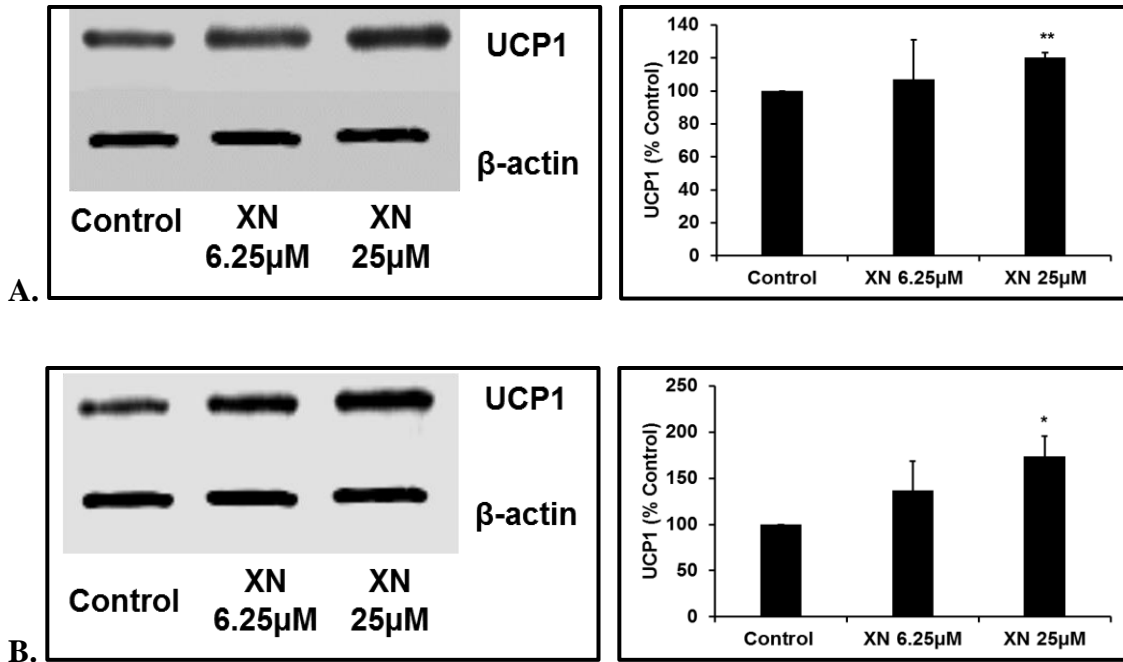


**Figure 26. XN-stimulated RAW264.7 cells indirectly beige 3T3-L1 adipocytes. A.**

Direct effects of mature 3T3-L1 adipocytes treated with varying concentrations of XN for

24 hours. **B.** Indirect effects of co-culturing of RAW264.7 macrophages and mature 3T3-

L1 adipocytes treated with XN for 24 hours. All data are presented as mean  $\pm$  SEM.

Statistical significance between control and treatment groups is represented as \* $P < 0.05$ ,

\*\*  $P < 0.01$ .

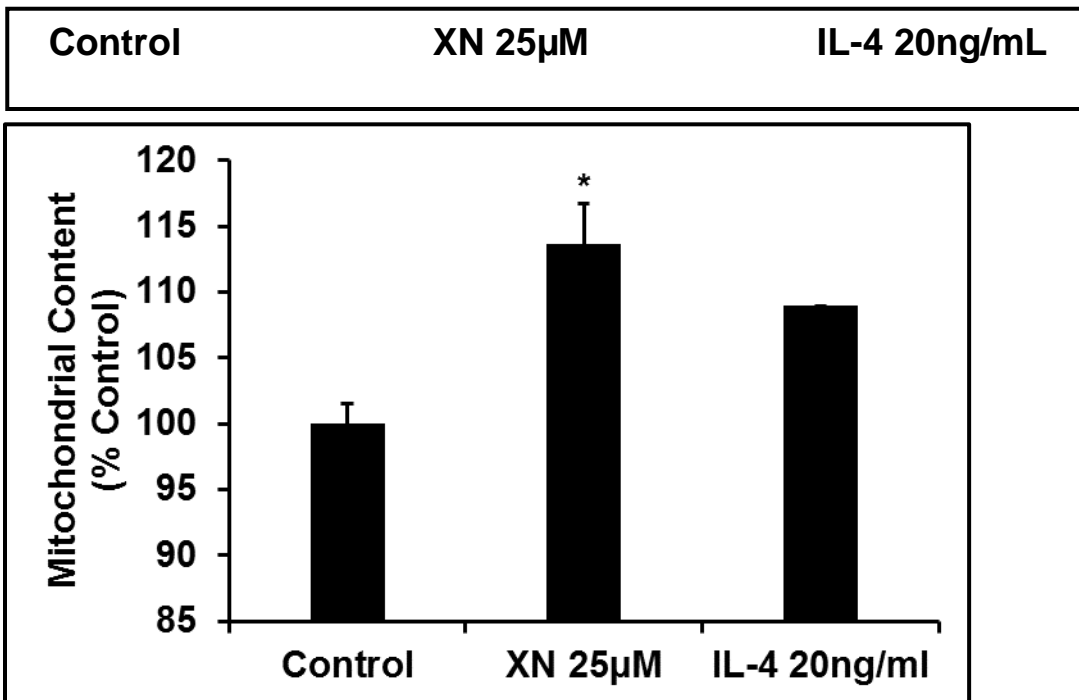
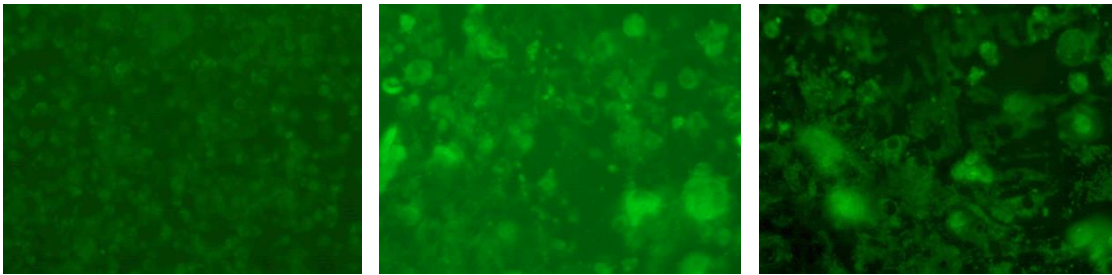


**Figure 27. Mitochondrial content in mature 3T3-L1 adipocytes co-cultured with XN stimulated RAW264.7 macrophages.** All data are presented as mean  $\pm$  SEM. Statistical significance between control and treatment groups is represented as \* $P < 0.05$ .

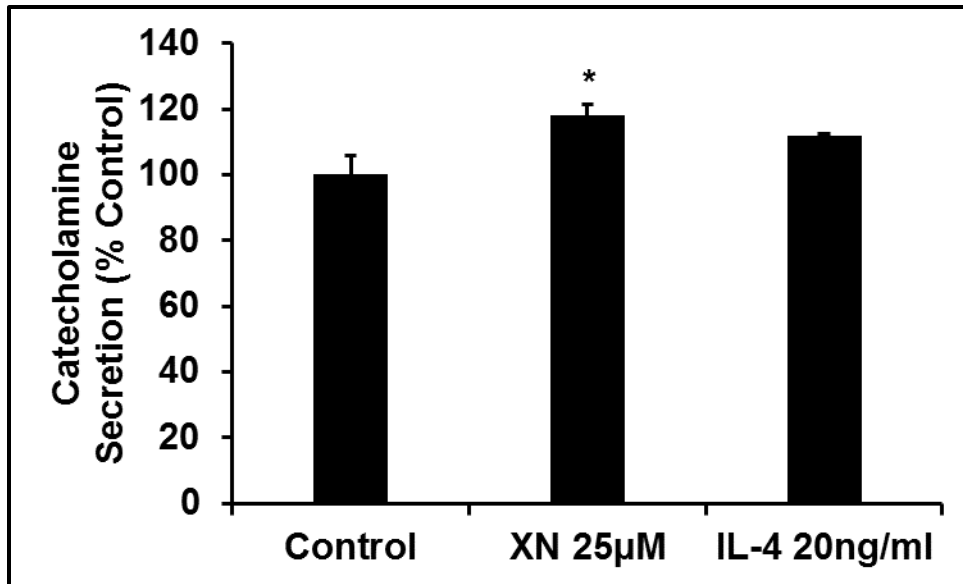


**Figure 28. Catecholamine secretion levels in XN treated macrophages co-cultured with 3T3-L1 adipocytes.** All data are presented as mean  $\pm$  SEM. Statistical significance between control and treatment groups is represented as \*  $P < 0.05$ .

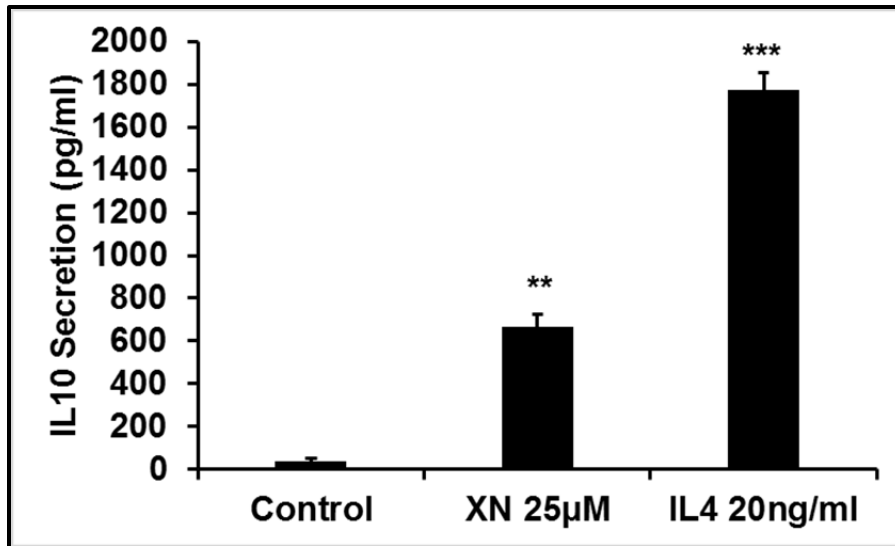


**Figure 29. Effect of XN treated macrophages co-cultured with 3T3-L1 adipocytes on IL-10 secretion levels.** All data are presented as mean  $\pm$  SEM. Statistical significance between control and treatment groups is represented as \*\*  $P < 0.01$ , \*\*\*  $P < 0.001$ .

## **Chapter Five**

### **Conclusions**

Provided that obesity is a result of energy imbalance and chronic inflammation, WAT stores excess energy in the form of triglycerides. Phytochemicals that increase sympathetic nervous system activation to increase thermogenesis, increase brown/beige adipocyte proliferation, activate brown adipocytes, polarize macrophages towards the anti-inflammatory phenotype, or beige adipocytes, may alleviate adipose tissue dysfunction.

Research directed toward understanding the responsiveness of activated BAT to achieve and maintain energy homeostasis could provide novel anti-obesity therapies. Furthermore, targeting adipose tissue-specific inflammation could also supplement combating obesity. The present study offers novel insights into the role of the prenylated flavonoid XN in inducing the brown fat-like phenotype in 3T3-L1 adipocytes and the polarization of macrophages.

We have successfully demonstrated that XN induces the beige phenotype in 3T3-L1 adipocytes and drives thermogenic programming as witnessed by the significant elevation of brown/beige-fat specific proteins such as UCP1, CIDE-A, TBX-1, ZIC1, and PGC-1 $\alpha$ . It has been identified that beige adipocytes, not brown adipocytes, express TBX-1 [102]. This led us to the conclusion that XN has a role in inducing the beige phenotype. Additionally, XN upregulated the expression of the brown/beige adipocyte specific UCP1 protein, confirming the acquired brown-like phenotype in XN-stimulated 3T3-L1 adipocytes.

Once white adipocytes are transdifferentiated into beige adipocytes, these beige adipocytes acquire large amounts of mitochondria [103]. Our data demonstrates that XN increased mitochondrial biogenesis, as evidenced by the upregulation of PGC-1 $\alpha$ , a transcriptional regulator of mitochondrial biogenesis and function, and MitoTracker™ green assay. XN also appeared to decrease adipogenesis and promote lipolysis as witnessed by a decrease in lipid content and lipid droplet size, therefore reducing adiposity.

Macrophages are regarded as prominent mediators in obesity. Their sub-populations, M1 and M2, could have deleterious or protective functions in the inflammatory response depending on their microenvironment. Manipulation of the ratio of M1/M2 macrophages could have a therapeutic effect in the treatment of obesity.

In the present study, we demonstrated that XN possesses immunomodulatory and anti-inflammatory activities in RAW264.7 macrophages. XN upregulated the classical M2 marker, arginase – 1, in RAW264.7 cells. Additionally, XN induced the secretion of catecholamines and IL-10 from RAW264.7 cells, suggesting that monocytes have been promoted towards the anti-inflammatory phenotype. XN prevented the polarization of monocytes towards the pro-inflammatory phenotype as evidenced by the attenuation of IFN- $\gamma$ -induced iNOS expression and nitrite release.

The activation of AMPK is crucial in maintaining energy homeostasis. Our data show that XN significantly upregulates the expression of activated AMPK in both 3T3-L1 adipocytes and RAW264.7 cells and its effect was abolished by inhibition with dorsomorphin of AMPK. Further, using the AMPK activator, AICAR, and inhibitor, dorsomorphin, we found that XN-induced beiging of 3T3-L1 adipocytes and anti-inflammatory polarization of macrophages is mediated through the activation of the AMPK signaling pathway.

In conclusion, our findings suggest that XN possesses multi-faceted anti-obesity effects, making for an attractive pharmacological drug therapy for the treatment and prevention of obesity. Our *in vitro* data provides novel evidence of XN's role in the modulation of improving the metabolic profile.



## References

1. Villarroya, F., et al., *Brown adipose tissue as a secretory organ*. Nature Reviews Endocrinology, 2016.
2. Wu, J., et al., *Beige Adipocytes Are a Distinct Type of Thermogenic Fat Cell in Mouse and Human*. Cell, 2012: p. 366-376.
3. Rao, R.R., et al., *Meteorin-like Is a Hormone that Regulates Immune-Adipose Interactions to Increase Beige Fat Thermogenesis*. Cell, 2014: p. 1279-1291.
4. Liu, M., et al., *Pharmacological Profile of Xanthohumol, a Prenylated Flavonoid from Hops (*Humulus lupulus*)*. Molecules, 2015: p. 754-779.
5. *Obesity and Overweight: Fact Sheet*, in World Health Organization. 2016.
6. Wang, Y., et al., *Will All Americans Become Overweight or Obese? Estimating the Progression and Cost of the US Obesity Epidemic*. Obesity, 2008: p. 2323-2330.
7. Pi-Sunyer, F.X., *The Obesity Epidemic: Pathophysiology and Consequences of Obesity*. Obesity, 2002: p. 97S-104S.
8. *Adult Obesity Causes & Complications*, in Centers for Disease Control and Prevention. 2016.
9. Zhang, Y., et al., *Obesity: Pathophysiology and Intervention*. Nutrients, 2014: p. 5153-5183.
10. Luo, X., et al., *Cold-Induced Browning Dynamically Alters the Expression Profiles of Inflammatory Adipokines with Tissue Specificity in Mice*. International Journal of Molecular Sciences, 2016: p. 1-14.

11. Moreno-Navarrete, J.M. and J.M. Fernandez-Real, *Adipocyte Differentiation*, in *Adipose Tissue Biology*. 2012, Springer New York. p. 17-38.
12. Rayalam, S., M.A. Della-Fera, and C.A. Baile, *Phytochemicals and regulation of the adipocyte life cycle*. *European Journal of Cell Biology*, 2008. **19**(11): p. 229-236.
13. Lefterova, M.I. and M.A. Lazar, *New developments in adipogenesis*. *Trends in Endocrinology & Metabolism*, 2009: p. 107-114.
14. Reichert, M. and D. Eick, *Analysis of cell cycle arrest in adipocyte differentiation*. *Oncogene*, 1999: p. 459-466.
15. Sealy, C.H., K. Geiger, and H. Drexel, *Brown versus White Adipose Tissue: A Mini-Review*. *Gerontology*, 2012: p. 15-23.
16. Seale, P., et al., *PRDM16 controls a brown fat/skeletal muscle switch*. *Nature*, 2008: p. 961-967.
17. Harris, R.B.S., *Direct and indirect effects of leptin on adipocyte metabolism*. *Biochimica et Biophysica Acta (BBA) - Molecular Basis of Disease*, 2014: p. 414-423.
18. Yao, X., et al., *Recent progress in the study of brown adipose tissue*. *Cell & Bioscience*, 2011: p. 1-35.
19. Asano, H., et al., *Induction of Beige-Like Adipocytes in 3T3-L1 Cells*. *The Journal of Veterinary Medical Science*, 2014: p. 57-64.
20. Huh, J.Y., et al., *Crosstalk between Adipocytes and Immune Cells in Adipose Tissue Inflammation and Metabolic Dysregulation in Obesity*. *Molecules and Cells*, 2014: p. 365-371.

21. Wang, N., H. Liang, and K. Zen, *Molecular Mechanisms That Influence the Macrophage M1-M2 Polarization Balance*. *Frontiers in Immunology*, 2014.
22. Pesce, J.T., et al., *Arginase-1-Expressing Macrophages Suppress Th2 Cytokine-Driven Inflammation and Fibrosis*. *PLOS Pathogens*, 2009.
23. Daneschvar, H.L., M.D. Aronson, and G.W. Smetana, *FDA-Approved Anti-Obesity Drugs in the United States*. *The American Journal of Medicine*, 2016: p. 879.
24. Lone, J., et al., *Curcumin induces brown fat-like phenotype in 3T3-L1 and primary white adipocytes*. *The Journal of Nutritional Biochemistry*, 2016: p. 193-202.
25. Rayalam, S., et al., *Anti-Obesity Effects of Xanthohumol Plus Guggulsterone in 3T3-L1 Adipocytes*. *Journal of Medicinal Food*, 2009: p. 846-853.
26. Gerhauser, C. and N. Frank, *Xanthohumol, a new all-rounder?* *Mol Nutr Food Res*, 2005. **49**(9): p. 821-3.
27. Stevens, J.F. and J.E. Page, *Xanthohumol and related prenylflavonoids from hops and beer: to your good health!* *Phytochemistry*, 2004. **65**(10): p. 1317-30.
28. Zanolli, P. and M. Zavatti, *Pharmacognostic and pharmacological profile of Humulus lupulus L.* *J Ethnopharmacol*, 2008. **116**(3): p. 383-96.
29. Arczewska, M., et al., *The molecular organization of prenylated flavonoid xanthohumol in DPPC multibilayers: X-ray diffraction and FTIR spectroscopic studies*. *Biochim Biophys Acta*, 2013. **1828**(2): p. 213-22.
30. Hirata, H., et al., *Xanthohumol, a prenylated chalcone from Humulus lupulus L., inhibits cholesteryl ester transfer protein*. *Food Chem*, 2012. **134**(3): p. 1432-7.

31. Costa, R., et al., *Xanthohumol and 8-prenylnaringenin ameliorate diabetic-related metabolic dysfunctions in mice*. J Nutr Biochem, 2017. **45**: p. 39-47.
32. Nozawa, H., *Xanthohumol, the chalcone from beer hops (Humulus lupulus L.), is the ligand for farnesoid X receptor and ameliorates lipid and glucose metabolism in KK-A(y) mice*. Biochem Biophys Res Commun, 2005. **336**(3): p. 754-61.
33. Rayalam, S., et al., *Novel molecular targets for prevention of obesity and osteoporosis*. J Nutr Biochem, 2011. **22**(12): p. 1099-104.
34. Miranda, C.L., et al., *Xanthohumol improves dysfunctional glucose and lipid metabolism in diet-induced obese C57BL/6J mice*. Arch Biochem Biophys, 2016. **599**: p. 22-30.
35. Mulligan, J.D., et al., *Upregulation of AMPK during cold exposure occurs via distinct mechanisms in brown and white adipose tissue of the mouse*. J Physiol, 2007. **580**(Pt. 2): p. 677-84.
36. Wang, S., et al., *Resveratrol induces brown-like adipocyte formation in white fat through activation of AMP-activated protein kinase (AMPK) alpha1*. Int J Obes (Lond), 2015. **39**(6): p. 967-76.
37. D van Dam, A., et al., *Regulation of brown fat by AMP-activated protein kinase*. Trends in Molecular Medicine, 2015: p. 571-579.
38. Daval, M., F. Foufelle, and P. Ferre, *Functions of AMP-activated protein kinase in adipose tissue*. J Physiol, 2006. **574**(Pt 1): p. 55-62.
39. Gauthier, M.S., et al., *Decreased AMP-activated protein kinase activity is associated with increased inflammation in visceral adipose tissue and with whole-*

- body insulin resistance in morbidly obese humans. Biochem Biophys Res Commun*, 2011. **404**(1): p. 382-7.
40. Yang, Z., et al., *Macrophage alpha1 AMP-activated protein kinase (alpha1AMPK) antagonizes fatty acid-induced inflammation through SIRT1. J Biol Chem*, 2010. **285**(25): p. 19051-9.
41. Gustafson, B., *Adipose tissue, inflammation and atherosclerosis. Journal of Atherosclerosis and Thrombosis*, 2010. **17**(4): p. 332-41.
42. Weisberg, S.P., et al., *Obesity is associated with macrophage accumulation in adipose tissue. 2003. 112*(12).
43. Sag, D., et al., *Adenosine 5'-monophosphate-activated protein kinase promotes macrophage polarization to an anti-inflammatory functional phenotype. J Immunol*, 2008. **181**(12): p. 8633-41.
44. Tiraby, C., et al., *Acquirement of Brown Fat Cell Features by Human White Adipocytes. 2003. 278*.
45. Soloveva, V., et al., *Transgenic Mice Overexpressing the B1-Adrenergic Receptor in Adipose Tissue Are Resistant to Obesity. 1997. 11*(1).
46. Kopecky, J., et al., *Reduction of dietary obesity in aP2-UCP transgenic mice: physiology and adipose tissue distribution. 1996. 270*(5).
47. Ouellet, V., et al., *Outdoor Temperature, Age, Sex, Body Mass Index, and Diabetic Status Determine the Prevalence, Mass, and Glucose-Uptake Activities of 18F-FDG-Detected BAT in Humans. 2011. 96*(1).
48. Lidell, M.E., et al., *Evidence for two types of brown adipose tissue in humans. 2013. 19*.

49. Azhar, Y., et al., *Phytochemicals as novel agents for the induction of browning in white adipose tissue*. 2016. **13**(89).
50. Yang, J.-Y., et al., *Effect of xanthohumol and isoxanthohumol on 3T3-L1 cell apoptosis and adipogenesis*. 20017. **12**(11).
51. Mendes, V., et al., *Xanthohumol Influences Preadipocyte Differentiation: Implication of Antiproliferative and Apoptotic Effects*. 2008. **56**(24).
52. Luo, Z., et al., *AMPK, the metabolic syndrome and cancer*. 2005. **26**(2).
53. Song, X.M., et al., *5-Aminoimidazole-4-carboxamide ribonucleotide treatment improves glucose homeostasis in insulin-resistant diabetic (ob/ob) mice*. 2002. **45**.
54. Fryer, L.G., A. Parbu-Patel, and D. Carling, *The Anti-diabetic drugs rosiglitazone and metformin stimulate AMP-activated protein kinase through distinct signaling pathways*. *J Biol Chem*, 2002. **277**(28): p. 25226-32.
55. Lee, Y.S., et al., *Berberine, a natural plant product, activates AMP-activated protein kinase with beneficial metabolic effects in diabetic and insulin-resistant states*. *Diabetes*, 2006. **55**(8): p. 2256-64.
56. Vucicevic, L., et al., *AMP-activated protein kinase-dependent and -independent mechanisms underlying in vitro antiglioma action of compound C*. *Biochem Pharmacol*, 2009. **77**(11): p. 1684-93.
57. Salminen, A., J.M.T. Hyttinen, and K. Kaarniranta, *AMP-activated protein kinase inhibits NF- $\kappa$ B signaling and inflammation: impact on healthspan and lifespan*. 2011. **89**(7).
58. Zhang, B.B., G. Zhou, and C. Li, *AMPK: An Emerging Drug Target for Diabetes and the Metabolic Syndrome*. 2009. **9**(5).

59. Poudel, B., et al., *Dioscin inhibits adipogenesis through the AMPK/MAPK pathway in 3T3-L1 cells and modulates fat accumulation in mice*. 2014. **34**(5).
60. Townsend, K.L. and Y.-H. Tseng, *Brown fat fuel utilization and thermogenesis*. 2014. **25**(4).
61. Seale, P., et al., *Prdm16 determines the thermogenic program of subcutaneous white adipose tissue in mice*. 2011. **121**(1).
62. Fernandez-Marcos, P.J. and J. Auwerx, *Regulation of PGC-1alpha, a nodal regulator of mitochondrial biogenesis*. *Am J Clin Nutr*, 2011. **93**(4): p. 884S-90.
63. Harms, M. and P. Seale, *Brown and beige fat: development, function and therapeutic potential*. *Nat Med*, 2013. **19**(10): p. 1252-63.
64. Fogarty, S. and D.G. Hardie, *Development of protein kinase activators: AMPK as a target in metabolic disorders and cancer*. 2010. **1804**(3).
65. Viollet, B., et al., *AMPK inhibition in health and disease*. 2010. **45**(4).
66. Musi, N. and L.J. Goodyear, *Targeting the AMP-activated protein kinase for the treatment of type 2 diabetes*. 2002. **2**(2).
67. Hardie, D.G., *AMPK: a key regulator of energy balance in the single cell and the whole organism*. *Int J Obes (Lond)*, 2008. **32 Suppl 4**: p. S7-12.
68. Weisberg, S.P., et al., *CCR2 modulates inflammatory and metabolic effects of high-fat feeding*. *J Clin Invest*, 2006. **116**(1): p. 115-24.
69. Bonet, M.L., P. Oliver, and A. Palou, *Pharmacological and nutritional agents promoting browning of white adipose tissue*. 2013. **1831**.

70. Ahn, J., et al., *The anti-obesity effect of quercetin is mediated by the AMPK and MAPK signaling pathways*. *Biochem Biophys Res Communications*, 2008. **373**(4).
71. Ono, M. and K. Fujimori, *Antiadipogenic effect of dietary apigenin through activation of AMPK in 3T3-L1 cells*. 2011. **59**(24).
72. Yin, W., J. Mu, and M.J. Birnbaum, *Role of AMP-activated protein kinase in cyclic AMP-dependent lipolysis In 3T3-L1 adipocytes*. *J Biol Chem*, 2003. **278**(44): p. 43074-80.
73. Daval, M., et al., *Anti-lipolytic action of AMP-activated protein kinase in rodent adipocytes*. *J Biol Chem*, 2005. **280**(26): p. 25250-7.
74. Symonds, M., *Adipose Tissue Biology*. 2012, New York: Springer.
75. Chinetti-Gbaguidi, G. and B. Staels, *Macrophage polarization in metabolic disorders: functions and regulation*. 2013. **22**(5).
76. Nguyen, K.D., et al., *Alternatively activated macrophages produce catecholamines to sustain adaptive thermogenesis*. *Nature*, 2011. **480**(7375): p. 104-8.
77. Feng, X., et al., *Chrysin attenuates inflammation by regulating M1/M2 status via activating PPAR $\gamma$* . 2014. **89**(4).
78. Osborn, O. and J.M. Olefsky, *The cellular and signaling networks linking the immune system and metabolism in disease*. *Nat Med*, 2012. **18**(3): p. 363-74.
79. Sica, A. and A. Mantovani, *Macrophage plasticity and polarization: in vivo veritas*. *J Clin Invest*, 2012. **122**(3): p. 787-95.



80. Barnes, M.A., M.J. Carson, and M.G. Nair, *Non-traditional cytokines: How catecholamines and adipokines influence macrophages in immunity, metabolism and the central nervous system*. 2015. **72**(2).
81. Wallace, F.A., et al., *Dietary fats affect macrophage-mediated cytotoxicity towards tumour cells*. 2000. **78**.
82. Lee, I.-S., et al., *Anti-inflammatory activity of xanthohumol involves heme oxygenase-1 induction via NRF2-ARE signaling in microglial BV2 cells*. 2010. **58**.
83. Suganami, T., J. Nishida, and Y. Ogawa, *A paracrine loop between adipocytes and macrophages aggravates inflammatory changes: role of free fatty acids and tumor necrosis factor alpha*. *Arterioscler Thromb Vasc Biol*, 2005. **25**(10): p. 2062-8.
84. Wesiberg, S.P., et al., *CCR2 modulates inflammatory and metabolic effects of high-fat feeding*. 2006. **116**(1).
85. Arkan, M.C., et al., *IKK-b links inflammation to obesity-induced insulin resistance*. 2005. **11**.
86. Kanda, H., et al., *MCP-1 contributes to macrophage infiltration into adipose tissue, insulin resistance, and hepatic steatosis in obesity*. 2006. **116**(6).
87. Gordon, S. and P.R. Taylor, *Monocyte and macrophage heterogeneity*. 2005. **5**.
88. Kawanishi, N., et al., *Exercise training inhibits inflammation in adipose tissue via both suppression of macrophage infiltration and acceleration of phenotypic switching from M1 to M2 macrophages in high-fat-diet-induced obese mice*. 2010. **16**.

89. Zhao, F., et al., *Inhibitors of nitric oxide production from hops (Humulus lupulus L.)*. Biol Pharm Bull, 2003. **26**(1): p. 61-5.
90. Dong, J., et al., *Quercetin reduces obesity-associated ATM infiltration and inflammation in mice: a mechanism including AMPKalpha1/SIRT1*. J Lipid Res, 2014. **55**(3): p. 363-74.
91. Carreras, A., et al., *Effect of resveratrol on visceral white adipose tissue inflammation and insulin sensitivity in a mouse model of sleep apnea*. Int J Obes (Lond), 2015. **39**(3): p. 418-23.
92. Gao, S., et al., *Curcumin induces M2 macrophage polarization by secretion IL-4 and/or IL-13*. J Mol Cell Cardiol, 2015. **85**: p. 131-9.
93. Zhao, H., et al., *Isoliquiritigenin, a flavonoid from licorice, blocks M2 macrophage polarization in colitis-associated tumorigenesis through downregulating PGE2 and IL-6*. Toxicol Appl Pharmacol, 2014. **279**(3): p. 311-21.
94. Giri, S., et al., *5-aminoimidazole-4-carboxamide-1-beta-4-ribofuranoside inhibits proinflammatory response in glial cells: a possible role of AMP-activated protein kinase*. J Neurosci, 2004. **24**(2): p. 479-87.
95. Pilon, G., P. Dallaire, and A. Marette, *Inhibition of inducible nitric-oxide synthase by activators of AMP-activated protein kinase: a new mechanism of action of insulin-sensitizing drugs*. J Biol Chem, 2004. **279**(20): p. 20767-74.
96. Nath, N., et al., *5-aminoimidazole-4-carboxamide ribonucleoside: a novel immunomodulator with therapeutic efficacy in experimental autoimmune encephalomyelitis*. J Immunol, 2005. **175**(1): p. 566-74.

97. Bruun, J.M., et al., *Monocyte chemoattractant protein-1 release is higher in visceral than subcutaneous human adipose tissue (AT): implication of macrophages resident in the AT*. J Clin Endocrinol Metab, 2005. **90**(4): p. 2282-9.
98. Nakamura, K. and S.F. Morrison, *A thermosensory pathway that controls body temperature*. Nat Neurosci, 2008. **11**(1): p. 62-71.
99. Xu, L., et al., *Hypoxia-induced secretion of IL-10 from adipose-derived mesenchymal stem cell promotes growth and cancer stem cell properties of Burkitt lymphoma*. Tumour Biol, 2016. **37**(6): p. 7835-42.
100. Lumeng, C.N. and A.R. Saltiel, *Inflammatory links between obesity and metabolic disease*. J Clin Invest, 2011. **121**(6): p. 2111-7.
101. Qiu, Y., et al., *Eosinophils and type 2 cytokine signaling in macrophages orchestrate development of functional beige fat*. Cell, 2014. **157**(6): p. 1292-308.
102. Garcia, R.A., J.N. Roemmich, and K.J. Claycombe, *Evaluation of markers of beige adipocytes in white adipose tissue of the mouse*. Nutr Metab (Lond), 2016. **13**: p. 24.
103. Toh, S.Y., et al., *Up-regulation of mitochondrial activity and acquirement of brown adipose tissue-like property in the white adipose tissue of fsp27 deficient mice*. PLoS One, 2008. **3**(8): p. e2890.